Journal of Geophysical Research: Planets

RESEARCH ARTICLE
10.1029/2018JE005698

Origin of Earth's Water: Chondritic Inheritance Plus Nebular Ingassing and Storage of Hydrogen in the Core

Jun Wu[1,2], Steven J. Desch[1], Laura Schaefer[1], Linda T. Elkins-Tanton[1], Kaveh Pahlevan[1], and Peter R. Buseck[1,2]

[1]School of Earth and Space Exploration, Arizona State University, Tempe, AZ, USA, [2]School of Molecular Sciences, Arizona State University, Tempe, AZ, USA

Key Points:
- Nebular ingassing supplied ~1% of Earth's water budget, complementing seven to eight oceans' worth of chondritic contribution
- Iron hydrogenation in magma oceans sequestered hydrogen and fractionated its isotopes, requiring $\alpha < 0.92$ to explain the solar contribution
- Approximately 60% of Earth's hydrogen resides in the core and has low-D/H ratios (~130 times 10^{-6})

Supporting Information:
- Supporting Information S1
- Data Set S1

Correspondence to:
J. Wu,
junwu1@asu.edu

Citation:
Wu, J., Desch, S. J., Schaefer, L., Elkins-Tanton, L. T., Pahlevan, K., & Buseck, P. R. (2018). Origin of Earth's water: Chondritic inheritance plus nebular ingassing and storage of hydrogen in the core. *Journal of Geophysical Research: Planets*, *123*. https://doi.org/10.1029/2018JE005698

Received 23 MAY 2018
Accepted 19 SEP 2018
Accepted article online 9 OCT 2018

Abstract Recent developments in planet formation theory and measurements of low D/H in deep mantle material support a solar nebula source for some of Earth's hydrogen. Here we present a new model for the origin of Earth's water that considers both chondritic water and nebular ingassing of hydrogen. The largest embryo that formed Earth likely had a magma ocean while the solar nebula persisted and could have ingassed nebular gases. The model considers iron hydrogenation reactions during Earth's core formation as a mechanism for both sequestering hydrogen in the core and simultaneously fractionating hydrogen isotopes. By parameterizing the isotopic fractionation factor and initial bulk D/H ratio of Earth's chondritic material, we explore the combined effects of elemental dissolution and isotopic fractionation of hydrogen in iron. By fitting to the two key constraints (three oceans' worth of water in Earth's mantle and on its surface; and D/H in the bulk silicate Earth close to 150×10^{-6}), the model searches for best solutions among ~10,000 different combinations of chondritic and nebular contributions. We find that ingassing of a small amount, typically >0–0.5 oceans of nebular hydrogen, is generally demanded, supplementing seven to eight oceans from chondritic contributions. About 60% of the total hydrogen enters the core, and attendant isotopic fractionation plausibly lowers the core's D/H to ~130×10^{-6}. Crystallized magma ocean material may have D/H ≈ 110×10^{-6}. These modeling results readily explain the low D/H in core-mantle boundary material and account for Earth's inventory of solar neon and helium.

Plain Language Summary People have long had curiosity in the origin of Earth's water (equivalently hydrogen). Solar nebula has been given the least attention among existing theories, although it was the predominating reservoir of hydrogen in our early solar system. Here we present a first model for Earth's water origin that quantifies contribution from the solar nebula in addition to that from chondrites, the primary building blocks of Earth. The model considers dissolution of nebular hydrogen into the early Earth's magma oceans and reaction between hydrogen and iron droplets within the magma ocean. Such processes not only delivered countless hydrogen atoms from the mantle to the core but also generated an appreciable difference in hydrogen isotopic composition (2H/1H ratio) between the mantle and core. Fitting the model to current knowledge about Earth's hydrogen produces best combinations of nebular and chondritic contributions to Earth's water. We find that nearly one out of every 100 water molecules on Earth came from the solar nebula. Our planet hides majority of its water inside, with roughly two *oceans* in the mantle and four to five oceans in the core. These results suggest inevitable formation of water on sufficiently large rocky planets in extrasolar systems.

1. Introduction

The origin of Earth's water is an unsolved mystery (Drake, 2005; Elkins-Tanton, 2011; Genda, 2016; Marty & Yokochi, 2006; Morbidelli et al., 2012; O'Brien et al., 2018; Robert, 2001). Understanding this longstanding enigma is key to assessing the evolutionary history and modern structure of Earth and has implications for how much water Mars and other planets in the solar system accreted. It also constrains the likelihood that rocky exoplanets possess liquid water on their surfaces and are habitable. As water is one of the prerequisites to life's birth, the grand topic also bears fundamental importance to astrobiology.

A successful theory of how Earth acquired its water must explain both the amount and isotopic composition of hydrogen on Earth's surface and in its mantle. Because hydrogen is easily oxidized to form water, the origin of Earth's water is equivalent to the sources of Earth's hydrogen. In addition to the one *ocean* (≅1.5×10^{21} kg) of water on Earth's surface, another several oceans' worth of hydrogen as OH and H_2O are believed to reside

in Earth's mantle including the transition zone (Bercovici & Karato, 2003; Genda, 2016; Hirschmann, 2006; Mottl et al., 2007). The average D/H ratio of this water is approximately 150×10^{-6} (or − 37‰ in δD notation; Hallis, 2017). (Here following common usage, D refers to ^{2}H and H to ^{1}H; H_2 is of unspecified isotopic composition.)

The current consensus is that Earth acquired most its water by accretion of carbonaceous chondrite material, particularly CI-like chondrites, from beyond the snow line in the solar nebula (Alexander et al., 2012; Marty, 2012; Morbidelli et al., 2000; Sarafian et al., 2017). For example, Raymond et al. (2004) find it likely in their simulations of planetary accretion that Earth could have accreted a single planetary embryo of mass ~0.1 M_E and water content ~10 wt %, which would have provided Earth with many tens of oceans of water. This consensus is bolstered by the observation that structurally bound water in carbonaceous chondrites, on average, has bulk $D/H \approx (140 \pm 10) \times 10^{-6}$ ($\delta D \approx (-101 \pm 60)$‰; Robert, 2006), a reasonable match to the terrestrial value. Other sources are considered unlikely. Cometary water generally has higher D/H ratios, up to 300×10^{-6} (δD = +926‰; Altwegg et al., 2015; Hartogh et al., 2011; Robert, 2006), whereas solar nebula gas has $D/H \approx 21 \times 10^{-6}$ ($\delta D \approx -865$‰; Geiss & Gloeckner, 1998).

This consensus view implicitly makes two assumptions, which may or may not be justified. First, with few exceptions (Hirschmann et al., 2012; Ikoma & Genda, 2006; Sasaki, 1990; Sharp, 2017), most models discount the contributions to Earth's hydrogen from ingassing of nebular H_2 and H_2O. But in fact, it has long been recognized from noble gas isotopic ratios that Earth's interior contains some He and Ne contributed from the solar nebula (Harper & Jacobsen, 1996; Marty, 2012; Pepin, 1992). More recently, Hallis et al. (2015) reported $D/H \leq 122 \times 10^{-6}$ ($\delta D \leq -217$‰) in Baffin Island rocks with high $^{3}He/^{4}He$ that sample the deep mantle. They advocated a solar nebula origin for this hydrogen by appealing to adsorption of nebular hydrogen onto fractal grains during Earth's accretion, which can be regarded as a variant of ingassing mechanism. New developments in planet formation theories lend credence to the ingassing hypothesis.

Second, in noting the D/H match between chondrites and Earth, the consensus view presumes that the hydrogen in Earth's mantle and surface reflects the entirety of its hydrogen. In fact, Earth's core must contain a significant fraction (~7 wt %) of light elements such as silicon, oxygen, and sulfur (Hirose et al., 2013). This inventory may include hydrogen, although first-principles molecular dynamics calculations yield opposing and controversial conclusions about the amount of hydrogen that can match seismic data (Caracas, 2015; Umemoto & Hirose, 2015). Wood et al. (2006) suggested its presence at the ~0.1 wt % level in the core based on geochemical grounds, enough hydrogen to supply ~12 oceans' worth of water. Likewise, McDonough (2003) estimated ~0.06 wt %, and Zhang and Yin (2012) calculated ~0.02 wt % hydrogen in the core. In contrast, Clesi et al. (2018) recently argued for much lower hydrogen contents in the cores of terrestrial planets based on the low hydrogen solubility that they measured in iron quenched from 5 to 20 GPa. However, their samples appear to have contained 3 to 7 wt % carbon, and carbon is known to significantly lower solubility of hydrogen in Fe_3C and related iron carbides (Litasov et al., 2016; Terasaki et al., 2014). Since Earth's core very likely contains $<$1 wt % carbon (Wood et al., 2013), the solubility of hydrogen may not be as low as Clesi et al. (2018) inferred (see section 5.1). We therefore think the other geochemical constraints to be reasonable and consider it likely that several oceans' worth of hydrogen, perhaps the majority of hydrogen, resides in the core, sequestered there as hydrogen in the mantle partitioned into metal blebs that then sank to the core. If this process were not accounted for, the total hydrogen content of Earth could be underestimated.

In contrast to the fact that various amounts of Earth's hydrogen have been proposed to have dissolved in its core (Genda, 2016, and references therein), little attention has been paid to any possible isotopic effect accompanying this hydrogen dissolution. In fact, a nonrare outcome when H_2 dissolves into various metals is that it isotopically fractionates such that the light hydrogen enters the metal, raising the D/H ratio in the surrounding medium (Andreev & Magomedbekov, 2001). To the extent that hydrogen is sequestered in Earth's core, the D/H ratio of the mantle may be higher than the bulk Earth, which would then demand that Earth must have also accreted an isotopically light component, which could have been ingassed solar nebula H_2 or H_2O. If this process were not accounted for, the isotopic composition of hydrogen in the bulk Earth could be mistakenly equated with that of the hydrogen remaining in the mantle.

In recognition of the facts that ingassing may be more plausible than previously thought and that both ingassing and storage of hydrogen in the core may alter the D/H ratio of Earth's water, we propose a new model for the origin of Earth's water. In section 2 we outline the hypothesis on which the model is based, which is that the planetary embryos comprising Earth brought chondritic water and that the largest of Earth's embryos

grew large enough within the lifetime of the solar nebula to ingas nebular H_2 and H_2O into its magma ocean. We then provide details of the model in section 3. In section 4 we present our results. In section 5 we discuss the implications of the model on the low-D/H ratio measured in material from near the core-mantle boundary and on Earth's inventory of neon and helium of nebular origin.

2. Hypothesis

2.1. Overview

Before delving into the details of the model, we provide an overview, illustrated in Figure 1. We hypothesize that Earth accreted from planetary embryos of various sizes, including smaller embryos of mass < 0.1 M_E, to a largest embryo with mass as large as 0.4 M_E. These embryos, we assume, formed from materials that initially had water contents characteristic of ordinary and enstatite chondrites, ~0.1 wt %, which would have provided Earth with roughly four oceans of H_2O. The embryos may also have included carbonaceous chondrite material with higher water content. These embryos are presumed to have formed quickly, perhaps via pebble accretion, on timescales less than a few million years, so that they formed within the lifetime of the solar nebula and were exposed to gas.

Due to radiogenic heating from ^{26}Al decay, these embryos quickly underwent metal-silicate differentiation. Small embryos of Ceres-like sizes may have lost part of their water content during and after differentiation. Nevertheless, such loss would probably have been only a small fraction of the total water content within all of Earth's accretion material. One reason for this possibility is that accretion of these Earth-forming embryos after their formation was rapid (Rubie et al., 2015), so that there was insufficient time for much water to have escaped from these small differentiated embryos. In addition, water would not have been necessarily lost from small differentiated bodies if they were beyond the snow line (Morbidelli et al., 2012).

As a result of differentiation within these embryos' mantles, H_2O reacted with Fe metal blebs to form iron hydrides that are expected to be stable above 4 GPa and 700 K (Fukai, 1984); when these blebs sank to the embryos' cores, this hydrogen was retained and sequestered owing to elevated conditions. We presume that this process fractionated hydrogen isotopes, putting relatively light hydrogen in the core and raising the D/H value of the mantle, an assumption consistent with the observation that the range of available D/H values of eucrite meteorites (Sarafian et al., 2014) is generally above that of carbonaceous chondrites (Alexander et al., 2012).

Assuming the largest planetary embryo reached ~0.3–0.4 M_E in mass during the lifetime of the solar nebula, we hypothesize that it accreted a protoatmosphere of H_2/He gas from the solar nebula, with surface pressure ~1–10 bar (Stökl et al., 2015). This protoatmosphere would have helped blanket the planet and sustain a magma ocean. We assume additional hydrogen, in the form of H_2 and H_2O, equivalent to a few tenths of an ocean, dissolved into the magma ocean, lowering its D/H ratio. Noble gases, especially He and Ne, also dissolved into the magma ocean during this stage.

After the solar nebula dissipated and the low-D/H magma ocean cooled and solidified, it presumably crystallized fractionally, creating late-solidifying cumulates that were denser than the average of the rocky mantle. The densest material would have sunk to the core-mantle boundary, whereas cumulates with intermediate density would have mixed with unmelted underlying mantle (Elkins-Tanton, 2011). This densest, Fe-enriched, very low D/H material, even if melted, is unlikely to have participated in mantle convection except as wisps. Therefore, during the following sequential collisions that progressively added mass to the largest embryo to form the final Earth, this material is expected to have survived multiple magma ocean events, even the possible whole-mantle remelting caused by the final, Moon-forming giant impact. As a result, it may reside today at the core-mantle boundary, perhaps associated with ULVZs (ultralow velocity zones) or LLSVPs (large low-shear-velocity provinces) (Brown et al., 2014).

Finally, Earth today would contain the following: a core sequestering over half of Earth's hydrogen, with relatively low D/H $\approx 130 \times 10^{-6}$ ($\delta D \approx -165‰$; see below); a mantle with most of the remaining approximately two oceans of hydrogen, with D/H $\approx 147 \times 10^{-6}$ ($\delta D \approx -56‰$; Clog et al., 2013); and a surface hydrosphere with one ocean of water and D/H $= 156 \times 10^{-6}$ ($\delta D = +1.5‰$; Lécuyer et al., 1998). In other words, between the mantle and surface there are approximately three oceans of water with average D/H $= 150 \times 10^{-6}$. If the mixing of crystallized magma ocean material were incomplete, the unmixed crystallized magma ocean material with very low D/H $\approx 109 \times 10^{-6}$ ($\delta D \approx -300‰$) would now reside at the core-mantle boundary.

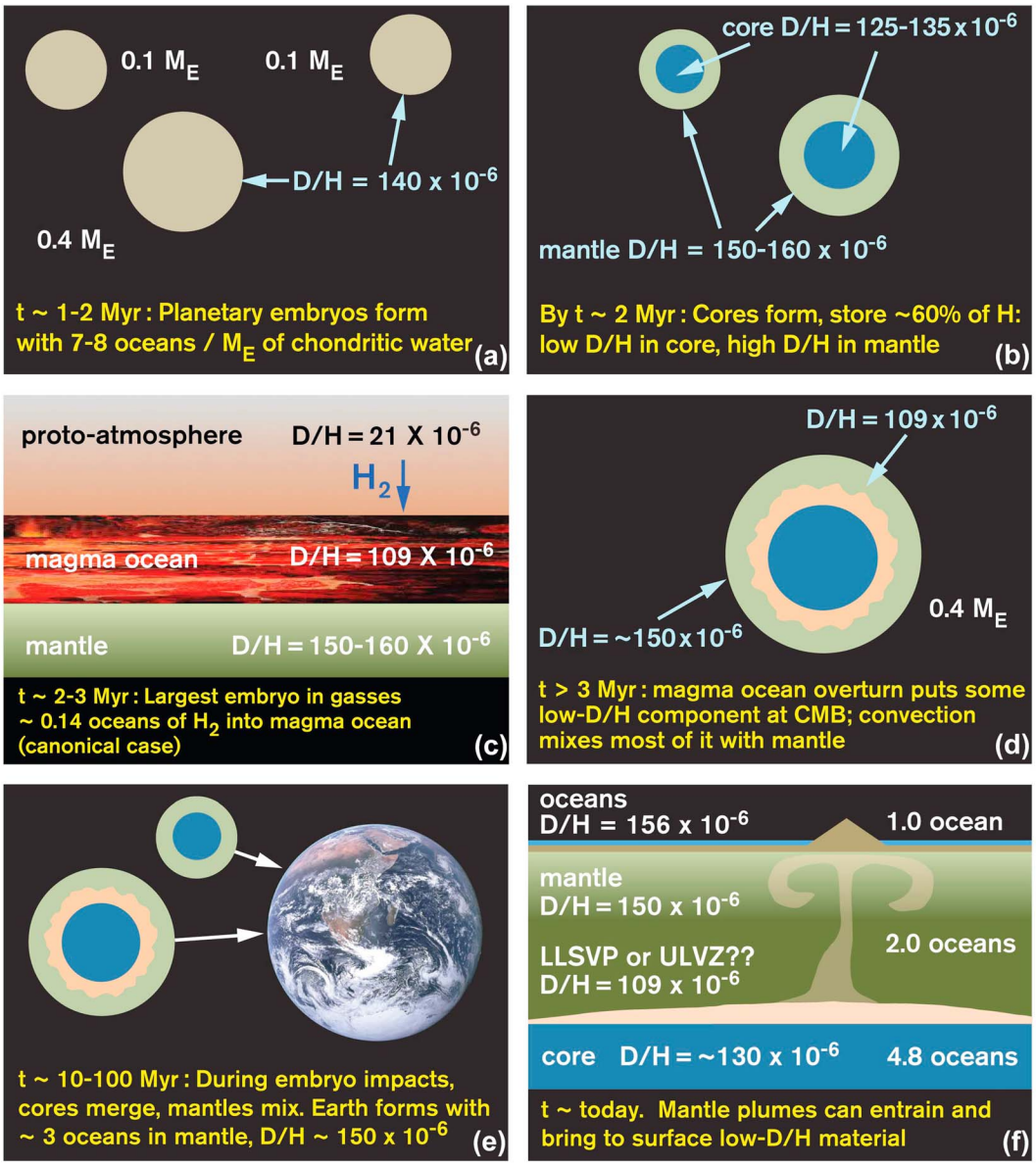

Figure 1. Overview of our model for how Earth acquired its water. (a) Earth accreted from embryos with chondritic levels of water concentrations and D/H ratios. (b) These embryos differentiated and stored relatively light hydrogen in their cores, raising the D/H of hydrogen in their mantles. (c) The largest embryo accreted a protoatmosphere and sustained a magma ocean into which nebular hydrogen diffused. (d) The largest embryo's magma ocean crystallized and overturned, mixing light hydrogen into the mantle, but incompletely. (e) As smaller embryos were accreted, their mantles joined the proto-Earth's mantle, and their cores merged with the proto-Earth's core. (f) Earth's mantle today contains approximately three oceans of water in its mantle and surface, with average D/H ≈ 150×10^{-6}, and ~4.8 oceans' worth of hydrogen in its core, with D/H ≈ 130×10^{-6}. Mantle plumes can sample low-D/H material from the core-mantle boundary. ULVZ = ultralow velocity zone; LLSVP = large low-shear-velocity province.

Mantle plumes originating at the core-mantle boundary could sample crystallized magma ocean material or mantle material that has isotopically exchanged with the core; in either scenario, this material could have D/H ≈ $100–130 \times 10^{-6}$ ($\delta D \approx -358$ to $-165‰$), consistent with the measurement of Hallis et al. (2015).

In the following sections we examine the model in greater detail.

2.2. Growth of Planetary Embryos

Until recently, the dominant paradigm for planet formation was hierarchical growth, in which kilometer-sized planetesimals collided and accreted over several million years to form Moon- to Mars-sized planetary

oligarchs or embryos, which subsequently collided with each other over the next 10–100 Myr to form the terrestrial planets (Morbidelli et al., 2012; Weidenschilling, 2000). Challenges for this class of models include the difficulty to explain coagulation of small particles past meter sizes to form planetesimals (Brauer et al., 2008) and the observation that asteroids and Kuiper belt objects have preferred diameters of 50–100 km (Bottke et al., 2010; Schlichting et al., 2009). This paradigm is now superseded by the discovery of two growth mechanisms: streaming instability, which can lead to rapid growth of ~100-km planetesimals from meter-sized particles or aggregates in $\ll$1 Myr (Johansen et al., 2007; Youdin & Goodman, 2005); and pebble accretion, by which very large planetesimals can accrete submeter particles and grow to embryo masses in $<$1 Myr (Ormel & Klahr, 2010; Lambrechts & Johansen, 2012; Levison et al., 2015, 2017).

These newly discovered mechanisms make plausible the idea that planetary embryos can grow very rapidly, just as radiometric dating and isotopic analyses of meteorites also strongly implicate rapid planet formation (Scherstén et al., 2006). Based on Mo and W isotopic anomalies, the solar nebula appears to have been divided into two isotopic reservoirs by the formation of Jupiter's $>$ 20-M_E core at $<$1 Myr after formation of calcium-rich, aluminum-rich inclusions (Kruijer et al., 2017). The formation of Mars has been dated to ~1.9 Myr after formation of calcium-rich, aluminum-rich inclusions, using both Hf-W dating (Dauphas & Pourmand, 2011) and the ^{60}Fe-^{60}Ni chronometer (Tang & Dauphas, 2014).

Not just small (0.1 M_E) but also larger (0.3–0.4 M_E) embryos appear capable of forming rapidly in the terrestrial planet-forming region. Previous N-body simulations showed growth to 0.4-M_E sizes at 1 AU by 2 Myr (Raymond et al., 2006, Figure 4). Recent simulations of pebble accretion indicate that in just 2 Myr the largest embryo at the locale near 1 AU, or the proto-Earth, was 0.3 M_E in mass, embedded in a distribution of smaller embryos, most with mass ~0.1 M_E (Levison et al. 2017, Figure 2).

The water content of these planetary embryos depends on whether they most strongly resembled enstatite chondrites, which are essentially water-free (Marty & Yokochi, 2006); ordinary chondrites, with typical (structurally bound) water fractions ~0.1 wt % (Alexander et al., 1989); or carbonaceous chondrites, with water contents ranging from ~1 wt % in CO and CV chondrites (Krot et al., 2015) to ~13 wt % in CI chondrites (Alexander et al., 2013). If Jupiter did divide the solar nebula into two reservoirs by opening the gap and restricting the flow of pebbles (Kruijer et al., 2017), then the embryos at 1 AU would have accreted material most strongly resembling ordinary and enstatite chondrites. Given that water fractions are much higher in carbonaceous chondrites than in enstatite and ordinary chondrites, Earth may nonetheless have accreted most of its water from carbonaceous chondrite material, a possibility suggested by Morbidelli et al. (2000) and others (Drake & Righter, 2002; O'Brien et al., 2006; Raymond et al., 2007; Sarafian et al., 2017).

Fits to Earth's elemental and isotopic compositions strongly suggest that it is indeed composed mostly of enstatite and ordinary chondrites (Alexander et al., 2012; Marty, 2012). For example, Dauphas et al. (2014) inferred that Earth's elemental abundances most strongly resemble a mix of 90.8 wt % enstatite chondrites, 6.8 wt % ordinary chondrites, 2.3 wt % CO and CV chondrites, and 0.2 wt % CI chondrites. We can reasonably assume that enstatite chondrites delivered essentially no water, ordinary chondrites were 0.1 wt % water and would have delivered about 0.3 oceans, CO and CV chondrites were 1 wt % water and would have delivered about 0.9 oceans, and CI chondrites were 13 wt % water and would have delivered 1.0 oceans. Using these numbers, carbonaceous chondrites contributed at least 86% of Earth's water, and perhaps more: There is evidence that the CO and CV chondrite parent bodies accreted even more water but subsequently dehydrated (Krot et al., 2015). Indeed, such a scenario is compellingly supported by mixing calculations based on elemental and isotopic measurements from angrite materials (Sarafian et al., 2017). Accretion of material elementally and isotopically similar to these carbonaceous chondrites (Robert, 2003), but with say 5 wt % water, or accretion of just 1% CI chondrite material, could have provided Earth $>$10 oceans of water, with ordinary chondrites contributing only a small fraction of that.

On average, the bulk isotopic composition of carbonaceous chondrites is D/H $\approx (140 \pm 10) \times 10^{-6}$ (Robert, 2006), and Earth might be assumed to start with this isotopic composition if carbonaceous chondrites dominated its water. More precisely, different chondrites vary in their bulk D/H ratios: ~170×10^{-6} (δD ~ + 91‰) in CI chondrites, ~150×10^{-6} in CO chondrites, ~160×10^{-6} (δD ~ + 27‰) in CV chondrites, and ~400×10^{-6} (δD ~ + 1568‰) in ordinary chondrites (Alexander et al., 2012). The mix of carbonaceous chondrites advocated by Dauphas et al. (2014) has an average ratio D/H $\approx$ 150–160×10^{-6}. Contributions from ordinary chondrites could raise the average D/H ratio of Earth.

We assume that Earth accreted from a variety of planetary embryos ranging in mass from <0.1 M_E, to a largest embryo 0.3–0.4 M_E. These embryos all formed by ~2 Myr, while nebula gas was present. Most of the embryos were relatively dry, with perhaps <0.1 wt % H_2O, equivalent to no more than four oceans, and probably much less. Accretion of a few percent carbonaceous chondrite material (Albarede et al., 2013; Alexander, 2017; Alexander et al., 2012; Dauphas, 2017; Dauphas et al., 2014; Marty, 2012; Warren, 2011) could have delivered an additional few to tens of oceans of water. We consider cases in which Earth ultimately inherited a mass $M_{chond} \approx 5$–25 oceans of *chondritic* water, dominated by contributions from carbonaceous chondrites. For this range of chondritic water inventory, generally no more than a few percent of it is believed to have been supplied by the *late veneer*; otherwise, the expected Earth-Moon isotopic match in oxygen isotopes would have been disrupted by accretion of excessive water to Earth after the Moon-forming giant impact (Greenwood et al., 2018). Furthermore, we consider this chondritic water to have D/H ratio between 130×10^{-6} and 170×10^{-6}, with D/H $\approx 140 \times 10^{-6}$ most likely.

2.3. Core Formation and Hydrogen Sequestration

Largely because of heating from radioactive decay, the planetary embryos experienced core-mantle differentiation caused by metal-silicate segregation that started as early as a few 0.1 Myr (Scherstén et al., 2006). Radiometric dating shows the parent bodies of iron meteorites underwent differentiation in <1 Myr (Kleine et al., 2002; Yoshino et al., 2003). Before temperatures adequate for differentiation were reached, the embryo interiors were sufficiently hot to release H_2O bound in hydrated minerals and phyllosilicates and also hydrogen in organic compounds (Mason, 1963; McNaughton et al., 1981). As H_2O reacted with Fe metal, it created FeO and, as an intermediate step, H_2. At high pressures and temperatures characteristic of the interiors of Mercury-sized bodies that have >0.05-M_E masses, the chemical affinity between iron and hydrogen is significantly enhanced (Fukai, 2005), which drove the dissolution of H_2 in the liquid iron droplets and formation of iron hydrides, FeH_x (Fukai, 1984; Hirschmann, 2012; Ohtani et al., 2005). Metal-silicate differentiation and sinking of iron droplets therefore provided a seemingly efficient mechanism for delivering hydrogen to the core.

We assume the dissolution of H_2 into FeNi blebs at all times reflected local chemical equilibrium, as the metal blebs in enstatite and ordinary chondrites are commonly small with an average size below 1 mm (Kuebler et al., 1999; Schneider et al., 2003), which is small enough for rapid chemical reaction and isotopic exchange. These blebs continued to interact and equilibrate with the mantle until they sank to the core and were incorporated there. The amount of hydrogen sequestered in the core therefore reflects metal-silicate equilibrium at the temperatures and pressures relevant to the core-mantle boundary of each embryo: ~2500 K and ~20 GPa for 0.1-M_E embryos, ranging up to ~3500 K and ~60 GPa for embryos as large as 0.4 M_E (Schaefer et al., 2017).

We estimate the solubility of hydrogen into FeNi metal droplets at these pressures and temperatures, as follows. H_2O dissolved in the silicate mantle would have reacted with the metal to form iron hydrides. Based on experimental data, at temperatures above ~1100 K and pressures above ~8.9 GPa the relevant reaction is

$$(x/2+1)\cdot\mathrm{Fe} + (x/2)\cdot\mathrm{H_2O} \rightarrow (x/2)\cdot\mathrm{FeO} + \mathrm{FeH}_x$$

(Ohtani et al., 2005), which can be decomposed into

$$(x/2)\cdot\mathrm{Fe} + (x/2)\cdot\mathrm{H_2O} \rightarrow (x/2)\cdot\mathrm{FeO} + (x/2)\cdot\mathrm{H_2}$$

and

$$\mathrm{Fe} + (x/2)\cdot\mathrm{H_2} \rightarrow \mathrm{FeH}_x$$

(Fukai, 1984). The governing step is the second reaction, in which dissolved H_2 with an effective pressure P_{H_2} dissolves in the iron.

For $P_{H_2} < 10$ MPa, Sieverts' law for gas solubility in metals applies, and the equilibrium molar concentration of H atoms in the metal is

$$c_H = (P_{H_2}/P_0)^{1/2} \cdot \exp\left[\left(-\Delta H^\circ + T\cdot\Delta S^\circ\right)/(R\cdot T)\right].$$

Here $\Delta H°$ and $\Delta S°$ are the enthalpy and entropy, respectively, for dissolution of hydrogen into iron at reference pressure $P_0 = 1$ bar and Kelvin temperature T, and $R = 8.314$ J·mol^{-1}·K^{-1} is the universal gas constant. We use $\Delta H° = +31.8$ kJ/mol and $\Delta S° = -38.1$ J·mol^{-1}·K^{-1}, appropriate for dissolution of H atoms into liquid iron (Fromm & Hörz, 1980).

As a typical example, if the concentration of H_2O were 1,000 ppm (a plausible value, equivalent to about three oceans of water dissolved in Earth's mantle), we estimate $P_{H_2} \approx 6.4$ MPa and $c_H \approx 0.031$ in iron droplets at the core-mantle boundary in a 0.4-M_E embryo, or $P_{H_2} \approx 4.0$ MPa and $c_H \approx 0.014$ for a 0.1-M_E embryo (arbitrarily assuming a lower mantle density of 3500 kg/m^3 for both). These estimates correspond to mass fractions of hydrogen in the core of 0.055 wt % for a 0.4-M_E embryo and 0.025 wt % for a 0.1-M_E embryo. These values compare favorably to other estimates for the equilibrium hydrogen mass fraction in Earth's core or ~0.06 wt % (McDonough, 2003) and ~0.02 wt %, respectively (Zhang & Yin, 2012), but at least 1 order of magnitude lower than the range of hydrogen content that was summarized by Genda (2016).

Earth's core has a ~10 wt % density deficit (Birch, 1952). With mass fractions ~0.025–0.055 wt %, hydrogen would be a minor species compared to other alloying elements such as oxygen, silicon, or sulfur (Badro et al., 2014; Hirose et al., 2013). Nevertheless, Earth's core, with mass ~0.32 M_E, would contain sufficient hydrogen to form three to six oceans. Even the well-known inhibitor of hydrogen dissolution in iron, that is, carbon, could also have entered the core, its expected low concentration (<1 wt %) in the core would have played a restrained role in depressing the hydrogen content therein. We conclude that a significant fraction, perhaps more than half, of Earth's hydrogen resides in its core.

The dissolution of hydrogen into metal droplets would have been isotopically selective, fractionating the hydrogen isotopes. Owing to the instability of iron hydrides at the low pressures at which mass spectrometry is possible, no measurements of this fractionation have been successful (Iizuka-Oku et al., 2017). However, based on hydrogen dissolution into proxies at low pressures, we expect the light isotopes of hydrogen to have been selectively taken up by the metal.

The key parameter quantifying this effect is the isotopic fractionation factor, α, by which hydrogen partitions between iron melt and surrounding silicate mantle:

$$\begin{aligned}\alpha &= (\mathrm{D/H})_{\mathrm{iron}}/(\mathrm{D/H})_{\mathrm{mantle}} \\ &= \left[(\mathrm{D/H})_{\mathrm{iron}}/(\mathrm{D/H})_{\mathrm{H_2}}\right] \times \left[(\mathrm{D/H})_{\mathrm{H_2}}/(\mathrm{D/H})_{H_2O}\right] \times \left[(\mathrm{D/H})_{H_2O}/(\mathrm{D/H})_{\mathrm{mantle}}\right].\end{aligned}$$

The H_2-H_2O fractionation factor can be extrapolated from calculated results of Richet et al. (1977), which yields $\ln[(\mathrm{D/H})_{H_2O}/(\mathrm{D/H})_{H_2}] = 2.22 \times 10^5/T^2$, and likewise the H_2O-mantle fractionation factor obtained by fitting experimental data of Dalou et al. (2015), which yields a linear trend line $\ln[(\mathrm{D/H})_{H_2O}/(\mathrm{D/H})_{\mathrm{mantle}}] = 1.56 \times 10^5/T^2$. Accordingly, we argue the product of the second two factors, $[(\mathrm{D/H})_{H_2}]/(\mathrm{D/H})_{H_2O}]\cdot[(\mathrm{D/H})_{H_2O}/(\mathrm{D/H})_{\mathrm{melt}}]$, is close to unity, that is, ~0.99. We identify α solely with the first fractionation factor, between what is effectively H_2 dissolved in the silicate and hydrogen in the metal.

Metals for which $\alpha < 1$ are said to exhibit a negative isotope effect. For γ-Fe metal, $\alpha = 0.972$, apparently independent of temperature (Heumann & Primas, 1966). For Ni, which shares many properties with Fe, $\alpha = 0.926\cdot\exp(-25.6\ \mathrm{K}/T)$ for temperatures 673–973 K and $P_{H_2} = 0.1$ MPa (Hawkins, 1953). Extrapolating beyond this range, we estimate $\alpha = 0.917$ at 2500 K. For Pd, $\alpha = 0.805\cdot\exp(372\ \mathrm{K}/T)$ or about 0.934 at 2500 K (Lacher, 1937). Thus, it is reasonable to assume that $\alpha < 1$, possibly $\alpha \approx 0.90$, for H_2 dissolving into FeNi liquid droplets at 2500–3500 K and low pressure. Considering that the pressure effect is generally small for isotopic fractionation, we expect that these numbers would be only slightly different at high pressure relevant to mantle conditions. In our calculations we consider a wide range of values, $0.75 < \alpha < 0.95$.

A value of $\alpha \approx 0.90$ or lower would lead to significant isotopic changes during hydrogen sequestration. Assuming half of Earth's hydrogen remained in the mantle and half were sequestered in its core (and neglecting changes in the isotopic reservoirs during core formation), we estimate that the D/H ratio in the mantle would be raised by a factor of 2/1.90, from 140×10^{-6} to 147×10^{-6}, whereas the D/H ratio in the core would be 0.90 times that of the mantle, or D/H = 133×10^{-6} ($\delta D = -146‰$).

2.4. Ingassing of Hydrogen Into a Magma Ocean

In addition to core formation, a planetary embryo's inventory of hydrogen and its isotopic composition can be affected by ingassing of nebular H_2 if the embryo's magma ocean was exposed to a protoatmosphere accreted from the solar nebula while nebular gas was still present. The frequency of stars with protoplanetary disks appears to fall off with stellar age, with a *half-life* of about 3 Myr (Haisch et al., 2001; Ribas et al., 2015). The ages of chondrules, which formed in the presence of nebular gas, suggest that gas was present in the terrestrial planet-forming region for at least 3 Myr (Villeneuve et al., 2009). Embryos that formed within the

first 3 Myr or so of disk evolution could have accreted nebular gas. The formation of Mars (~0.1 M_E) is radiometrically dated to have taken <2 Myr (Dauphas & Pourmand, 2011; Tang & Dauphas, 2014), meaning that it, and likely other planetary embryos, formed while nebular gas was present.

Exoplanets provide further, strong evidence that embryos grow large during the presence of nebular gas. Observations of rocky exoplanets convincingly suggest that those with masses above 5 Earth masses (>1.5 Earth radii) have H_2/He atmospheres that are a few percent or more of the planet's mass (Rogers, 2015; Weiss & Marcy, 2014).

Calculations indicate that smaller, planetary embryos would have possessed at least transient protoatmospheres of surface pressures ~1–10 bar (Stökl et al., 2015). These atmospheres would not necessarily have persisted after the disk was gone. While a 0.4-M_E embryo could have accreted a ~10-bar protoatmosphere and retained it against escape for ~10 Myr after the disk dissipated, 0.1-M_E embryos are predicted to have accreted much less substantial atmospheres and could not have retained them for more than 1–10 years after dissipation of the nebula (Stökl et al., 2015). During the >3-Myr lifetime of the solar nebula, though, these protoatmospheres would have been present around planetary embryos. If the embryos also possessed magma oceans—an outcome enabled by the blanketing effects of a protoatmosphere—then H_2, He, Ne, etc. would have ingassed from the solar nebula into the magma ocean.

Magma oceans of varying dimensions likely occurred multiple times either on the surface or within the interior of planetary embryos, depending on the location of heat release and frequency of large impacts. In relatively small embryos ~0.1 M_E, radiogenic heat plus potential energy of sinking metal could have melted their interiors, forming internal magma oceans. As they grew, heat from accretional impacts may have increased sufficiently to melt their exteriors.

In larger embryos, ~0.4 M_E, impacts could have created large surface magma oceans. For example, a collision between a 0.1-M_E embryo and a 0.5-M_E proto-Earth is estimated to create a surface magma ocean of >700-km depth for a typical impacting speed (Tonks & Melosh, 1993). Alternatively, the accretion of ~10^3 Ceres-sized bodies in a short time presumably would have generated a similar mass of magma ocean. Such impacts may have taken place during the first ~2 Myr of the evolution of the solar nebula (e.g., Raymond et al., 2006). Depending on the sizes of the target embryo and impactors, a surface magma ocean could have been local, hemispheric, or global. This predicted coexistence of a surface magma ocean and nebula-originated protoatmosphere strongly implies ingassing, the dissolution of nebular gases into the underlying magma ocean, a scenario also recently investigated by Sharp (2017).

Assuming the persistence of magma oceans, we assess the amount of hydrogen that could be ingassed as follows. First, a ~10-bar H_2 atmosphere around a 0.4-M_E embryo has mass ~10^{21} kg, equivalent to approximately six oceans' worth of H_2O if the hydrogen could be oxidized. Only a fraction of this hydrogen could be ingassed, as the solubility of H_2 is limited. The equilibrium mass fraction of H_2 dissolved into a silicate melt is $xH_2 = 1 \cdot (P_{H_2}/10\ \text{bar})$ ppm under the typical redox conditions of an early magma ocean (Hirschmann, 2012). A 0.4-M_E embryo with a ~0.1-M_E magma ocean would ingas a negligible amount of H_2, the equivalent of <0.004 oceans of water. On the other hand, the solubility of H_2O in magma is much higher than that of H_2. The redox state of a magma ocean was such that P_{H_2O}/P_{H_2} in the protoatmosphere was likely between ~0.01 and 0.1, equivalent to a redox state 4 to 2 log units below the iron-wüstite (IW) buffer, or IW-4 to IW-2, at magmatic temperatures (Hirschmann, 2012). Here we assume that the equilibrium speciation in the protoatmosphere was $P_{H_2O}/P_{H_2} = 0.1$. The mass fraction of the mantle that could be ingassed H_2O is $x_{H_2O} = 1300 \cdot (P_{H_2O}/1\ \text{bar})^{1/2}$ ppm (Fricker & Reynolds, 1968), equivalent to 0.5 oceans of water. The actual amount that was ingassed would depend on the kinetics of how fast gas dissolved into the magma ocean, the mixing of material within the magma ocean, and the kinetics of replenishment of the protoatmosphere from the solar nebula.

We estimate that a few tenths of an ocean of H_2O would have ingassed into the magma ocean of the largest (~0.4 M_E) embryo. This ingassing of H_2O must have been a net effect after summation of the following processes involving dissolution, oxidation, outgassing, and ingassing:

$$H_2{}^{\text{protoatmosphere}}\ (g) \rightarrow H_2{}^{\text{magma}}\ (g)$$

$$H_2{}^{\text{magma}}\ (g) + O^{\text{magma}}\ (l) \rightarrow H_2O^{\text{magma}}\ (l)$$

$$H_2O^{magma}\ (l) \rightarrow H_2O^{protoatmosphere}\ (g)$$

$$H_2O^{protoatmosphere}\ (g) \rightarrow H_2O^{magma}\ (l)$$

Associated with the summed reaction is also isotopic fractionation of hydrogen, whose equilibrium constant is expected to be very close to 1 at typical surface temperatures of a magma ocean (Richet et al., 1977). Consequently, within the lifetime of magma oceans (<10 Myr), this ingassed water would reflect an isotopic composition close to that of the hydrogen-rich protoatmosphere, that is, D/H = 21×10^{-6}. This material would have mixed thoroughly in the convecting magma ocean. Mixing of 0.5 oceans, for example, of H_2O with D/H = 21×10^{-6} into a ~0.1-M_E magma ocean with water mass fraction 1,000 ppm and D/H = 140×10^{-6} would have yielded a higher mass fraction of water, ~2,250 ppm, and lower D/H ≈ 74×10^{-6} (δD ≈ −525‰). This material would not necessarily have mixed into the underlying mantle before the magma ocean crystallized.

2.5. Crystallization and Overturn of a Magma Ocean

The cumulate mantle that resulted from solidification of a magma ocean is likely to have been gravitationally unstable, that is, likely to have involved denser material overlying less dense material. Three processes could have produced an unstable density gradient: enrichment of the magma ocean liquids in heavy elements as fractional solidification progressed, increased density of materials near the surface because they contracted due to the colder temperatures there, and increased Fe/(Fe + Mg) in mafic materials near the end of solidification. The likelihood of an unstable density gradient in solidified magma oceans has been discussed by Schnetzler and Philpotts (1971), Hess and Parmentier (1995), Solomatov (2000), and Elkins-Tanton (2012), among others.

The relatively low viscosity of the warm, new cumulate pile would have allowed overturn in embryos up to the size of Mars, yielding gravitational stability in hundreds of thousands to just a few millions of years, depending upon the bulk composition and size of the planet (Scheinberg et al., 2014; Zaranek & Parmentier, 2004). The most compositionally dense material would remain at the bottom of the mantle, against the core, permanently resistant to thermal convection (Brown et al., 2014; Ohtani & Maeda, 2001), providing an opportunity to preserve isotopically light material from the crystallized magma ocean, potentially with D/H as low as ~109×10^{-6}, at the core-mantle boundary.

2.6. Subsequent Accretion of Embryos

The planetary embryos comprising Earth would have accreted and undergone metal-silicate differentiation, and the largest embryo would have ingassed nebular hydrogen before the solar nebula dissipated after ~3 Myr. Crystallization and overturn of the magma ocean are presumed to have been complete within a ~10-Myr timescale. Their atmospheres would have dissipated around this time. Even the largest (~0.4 M_E) embryos we consider here would have lost their atmospheres on ~10-Myr timescales (Stökl et al., 2015), but perhaps longer (Hamano et al., 2013). On ~10- to 100-Myr timescales the other embryos are expected to have collided with the largest embryo, which was the proto-Earth (e.g., Raymond et al., 2006). Hf-W dating of the Moon-forming impact shows the last ~0.1-M_E embryo was accreted by Earth by about 50–100 Myr (Kleine et al., 2009; Touboul et al., 2007). During each impact, the cores and mantles of the embryos and the proto-Earth would have mixed and merged.

Sequential collisions between the proto-Earth and other embryos over tens of million years would have mixed their mantle materials well, although perhaps not completely. Collisions of embryos with the proto-Earth would have produced magma oceans in which turbulent entrainment and violent convection of silicate magma were rapid during and after the collisions. At early stages, the collision-generated magma oceans could have been only local or hemispherical, but as the growing proto-Earth approached its final mass, creation of a massive magma ocean on a global scale through a giant impact like the Moon-forming event is conceivable.

The cores of the embryos, by virtue of their high density, would have merged with the proto-Earth's core. Classical models of core formation assume chemical equilibration between iron-rich metal and surrounding silicate magma ocean (Wade & Wood, 2005), which is probably true for collisions where the target body was relatively small or the impactor was undifferentiated. However, for a proto-Earth with mass > 0.6 M_E that collided with an embryo of mass > 0.06 M_E, the merged body likely experienced incomplete emulsification and chemical equilibration of the embryo's core, so that much of it merged directly with that of the proto-Earth without equilibration (Rubie et al., 2011). In fact, the extent of metal equilibration for the cores of large

impactors remains unclear (Dahl & Stevenson, 2010; Rubie et al., 2015). We consider both end-member scenarios of perfect mergers of cores and complete equilibration of embryo cores with the proto-Earth's mantle.

Even if complete melting of the proto-Earth's mantle occurred, there would not have been significant mixing with the surrounding mantle of any low-D/H material at the core-mantle boundary, which resulted from overturn of crystallized magma ocean material that experienced ingassing. Because of its higher density, this material would be expected to remain stagnant at the core-mantle boundary.

Earth's accretion may have extended into a late veneer period after the large impacts between these ~0.1 M_E and bigger embryos. A recent numerical simulation showed that pollution by the core disruption of a differentiated, Moon-sized impactor could have been responsible for the excessive HSE (highly siderophile elements) signatures in the current Earth's mantle (Genda et al., 2017). According to their results, most postcollision iron fragments of the impactor's core would have been temporarily ejected into space as ~10-m-sized blobs and then reaccreted to Earth's silicate mantle, suspending there for adequate chemical reactions to have supplied chondritic HSE inherited from the impactor. The proposed mechanism, even if having operated for HSE, is unlikely to have worked for hydrogen in our case.

As described in section 2.3, dissolution of hydrogen in iron is highly pressure sensitive, which is in contrast to strong affinity of HSE to iron at all pressure ranges within a planetary body. At the core conditions of a Moon-sized embryo, the iron would have held only a hydrogen abundance below 0.05 wt %, corresponding to a molar concentration $c_H \approx 0.01$ and translating into a rather small amount of hydrogen for the core of a 0.01-M_E embryo. Nevertheless, a more important reason for essentially no hydrogen pollution would have been rapid pressure release from several gigapascals to below 0.1 MPa due to core disruption. Immediately after the impactor's core was fragmented into ~10-m blobs, most of hydrogen dissolved in them would have quickly escaped so that c_H reduced to the order of 10^{-4} or even lower. Therefore, the residual trace hydrogen inherited from the impactor's core would have had only a negligible influence on the hydrogen signature of Earth's mantle.

3. Model

We calculate the masses and isotopic compositions of different reservoirs of water within the growing Earth, as follows.

We initialize the problem by considering one embryo having a mass 0.4 M_E, the other embryos having masses $M_p \sim 0.1$ M_E. Each is given an identical concentration of water $c_{H_2O} = M_{chond}/M_E$, where M_{chond} ranges from 5 to 25 oceans, with its D/H ratio, $(D/H)_{chond}$, ranging from 130×10^{-6} to 170×10^{-6}. In each embryo, we consider iron to melt and sink to form a core. We grow the core in N_{steps} steps, increasing its mass by M_{core}/N_{steps} at each step. Each core ultimately has a mass $M_{core} \approx 0.33\ M_p$, by assumption.

As the core grows, we keep track of the concentration and D/H ratio of hydrogen both in the mantle and in the core, by keeping track of the numbers of H and D atoms in both reservoirs. We start with zero H and D atoms in the core. In the mantle of each embryo with mass M_p, the initial numbers of H and D atoms are $N_H = M_{chond}\cdot(M_p/M_E)/[(m_H + m_O/2) + (D/H)_{chond}\cdot(m_D + m_O/2)]$ and $N_D = (D/H)_{chond}\cdot N_H$. At each step we calculate the concentration of hydrogen in the iron blebs sinking at that time, using the solubility equation $c_H = (P_{H_2}/P_0)^{1/2}\cdot\exp[(-\Delta H^\circ + T\cdot\Delta S^\circ)/(R\cdot T)]$, and using the values appropriate for (low-pressure) dissolution of hydrogen into liquid iron (Fromm & Hörz, 1980) and the D/H ratio of hydrogen in the blebs from our assumption about α. We calculate the instantaneous value of $P_{H_2} = (1/2)\cdot(N_H + N_D)\cdot(\rho/M_{mantle})\cdot k\cdot T$, where N_H and N_D are the numbers of H and D atoms in the mantle, ρ is the magma density (assumed to be 3,450 kg/m^3), M_{mantle} is the mass of the mantle, and k is the Boltzmann constant. We calculate the number of H and D atoms in the iron blebs as

$$dN_H = c_H\cdot(dM/m_{Fe})/\left[1 + (D/H)_{bleb}\right],$$

and

$$dN_D = dN_H\cdot(D/H)_{bleb},$$

where m_{Fe} is the mass of an Fe atom and $(D/H)_{bleb} = \alpha\cdot(D/H)_{mantle}$. As these H and D atoms are delivered to the core, they are added to the core's inventory and are subtracted from the mantle, changing the

concentration of hydrogen (and P_{H_2}), as well as $(D/H)_{mantle}$. We numerically integrate the concentrations and D/H ratios in the core and mantle. We find that $N_{steps} > 10^5$ is needed for numerical convergence.

Next, in the largest embryo, we add a mass of hydrogen sufficient to produce a mass M_{ingas} of water which has D/H = 21×10^{-6} and is assumed to mix with the mantle.

We then consider the accretion of the smaller embryos to the largest one. During each accretion, we assume that the mantles are immediately well mixed, leading to a new mantle with averaged hydrogen concentration and D/H ratio. We assume a fraction 1-q of the accreted core mixes immediately with the target core and the rest, q, mixes with the mantle. This metal fraction equilibrates with the mantle before sinking to the growing core. The sequestration of hydrogen is calculated in the same manner as before. We particularly consider the two end-members: $q = 0$ (perfect mergers of all cores) and $q = 1$ (perfect equilibration with mantle before core merger).

We consider 15 combinations of $(D/H)_{chond}$ (130, 140, 150, 160, and 170×10^{-6}) and α (0.75, 0.85, 0.95); for each we test 201×51 combinations of M_{chond} from 5 to 25 oceans, and M_{ingas} from zero to one ocean, using a 0.1-ocean and 0.02-ocean incremental step for M_{chond} and M_{ingas}, respectively. After each numerical integration, we calculate the number of oceans of water remaining in the mantle, N_{mantle}, as well as the D/H ratios in the core and mantle. We seek solutions that are the closest fit to our presumed inventory of $N_{mantle} = 3$ oceans of water in Earth's mantle (one ocean of which presumably is outgassed to the surface), with average D/H $\approx 150 \times 10^{-6}$. We assign an uncertainty of one ocean to the target amount of water in the mantle and an uncertainty of 2×10^{-6} to the D/H ratios of the mantle and surface and define a goodness-of-fit parameter

$$\chi^2 = (N_{mantle} - 3)^2/1^2 + \left[(D/H)_{mantle} - 150{\times}10^{-6}\right]^2/\left(2{\times}10^{-6}\right)^2.$$

For each value of $(D/H)_{chond}$ and α we seek the values of M_{chond} and M_{ingas} that minimize χ^2. Combinations that yield $\chi^2 < 1$ are considered solutions.

4. Results

We first consider the scenario of perfect merger between the cores of the proto-Earth and embryos. Under this condition, the fitting results for $(D/H)_{chond} = 140 \times 10^{-6}$ (the most likely value for chondritic material) and each α value are made into contour plots (Figure 2, left column). In these cases only a limited range of M_{chond} and M_{ingas} satisfies $\chi^2 < 1$. The shapes of the solution areas in the plots indicate that M_{ingas} is more tightly constrained than M_{chond}. This outcome is consistent with the fact that D/H of ingassed hydrogen differs from the observed mantle value much more significantly than chondritic hydrogen. Also evident is the dependence of M_{ingas} on α, which can be understood qualitatively in terms of the Rayleigh equation. The closer α is to 1, the less nebular ingassing is required to satisfy the fitting constraints. In comparison, M_{chond} of the solutions are relatively insensitive to the choices of α value and at least 1 order of magnitude greater than M_{ingas}. The right column in Figure 2 presents the similar contour plots when $(D/H)_{chond}$ equals the highest assumed value, namely, 170×10^{-6}. It is clear by comparison that, for the same value of α, the higher the value of $(D/H)_{chond}$ is, the more hydrogen must be ingassed to satisfy the isotopic constraints.

Table 1 lists the values of M_{chond}, M_{ingas}, M_{core}, $(D/H)_{core}$, M_{mantle}, and $(D/H)_{mantle}$, as well as the goodness of fit, χ^2, in the best solutions for all combinations of $(D/H)_{chond}$ and α that are considered. For example, for $(D/H)_{chond} = 140 \times 10^{-6}$ and $\alpha = 0.85$, $M_{chond} = 7.90$ oceans and $M_{ingas} = 0.14$ oceans. For this case, $M_{core} = 4.83$ oceans, meaning that the hydrogen in the core, if oxidized, could create 4.83 oceans' worth of water. The isotopic ratio of hydrogen in the core is then $(D/H)_{core} = 130 \times 10^{-6}$. The amount and isotopic ratio of average water in the mantle and surface are $M_{mantle} = 3.18$ oceans and $(D/H)_{mantle} = 150 \times 10^{-6}$, matching the constraints with a minimum goodness-of-fit parameter $\chi^2 = 0.04$.

In general, in a best solution $M_{core}/M_{mantle} \approx 1.5$, a ratio fixed by our assumed hydrogen solubility. As a result, $M_{chond} \approx 7$–8 oceans in order to match the presumed amount of water in the mantle and surface, which then determines the amount of hydrogen that must be ingassed, M_{ingas}, to match the isotopic constraints. It is larger for larger $(D/H)_{chond}$ and for smaller values of α. Across the considered inputs, M_{ingas} ranges from 0 to 0.46 oceans, with larger amounts corresponding to smaller α. For example, for $(D/H)_{chond} = 140 \times 10^{-6}$, a nonzero contribution from nebular hydrogen requires $\alpha < 0.92$, unless there exists an alternative mechanism for

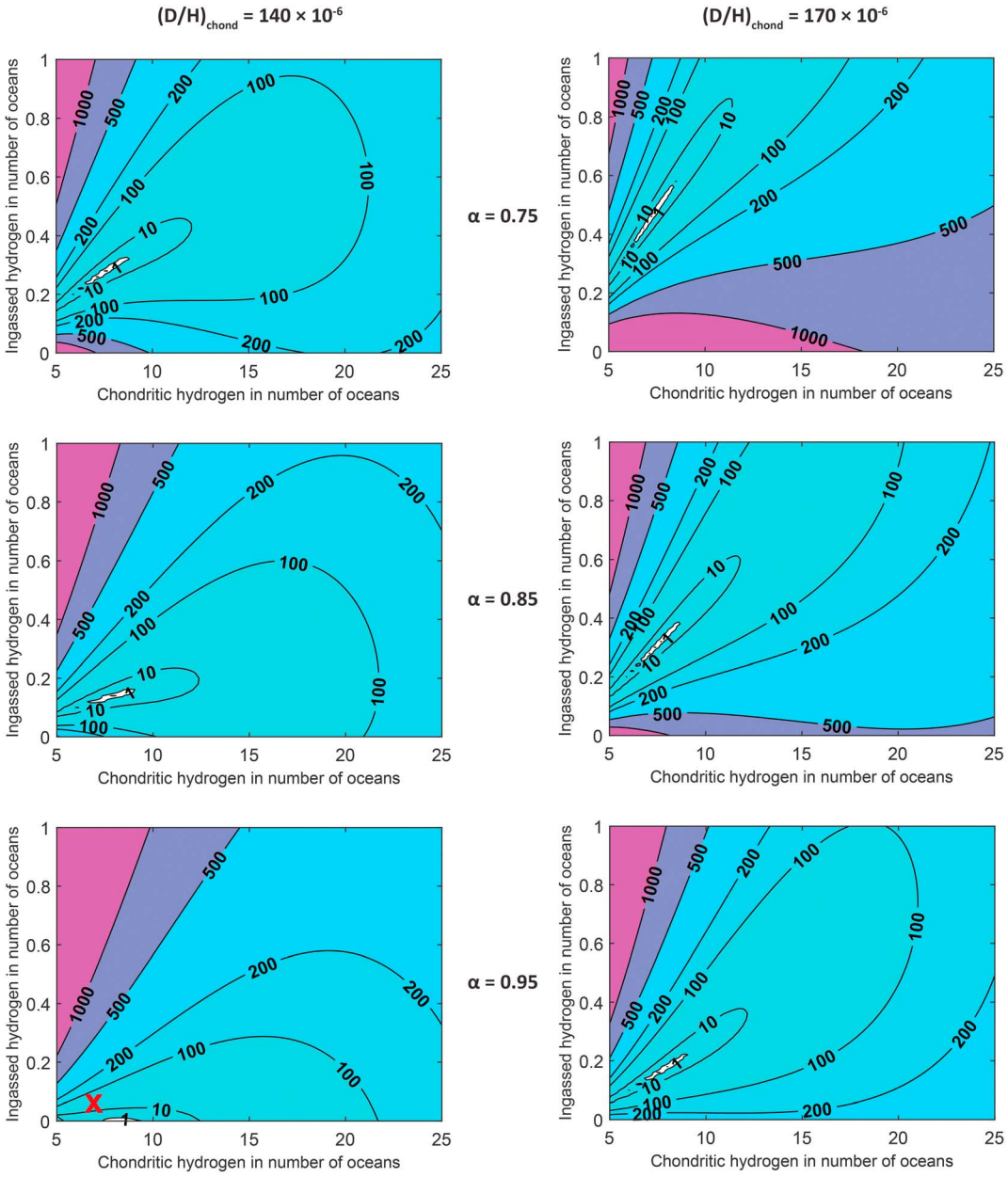

Figure 2. Goodness of fit, χ^2, as a function of M_{chond} and M_{ingas}, for the case $(D/H)_{chond} = 140 \times 10^{-6}$ (left column) and $(D/H)_{chond} = 170 \times 10^{-6}$ (right column). For each case three choices of α, that is, 0.75 (top row), 0.85 (middle row), and 0.95 (bottom row) are used to create the contour plots. Areas with relatively light colors correspond to fitting results with relatively small χ^2, and only those results within the contour line $\chi^2 = 1$ are considered possible solutions, as highlighted in the white-colored, strip-shaped area near the bottom left corner of each panel. A favored result ($M_{chond} = 7$ oceans, $M_{ingas} = 0.06$ oceans) that is based on the most likely input parameters, that is, $(D/H)_{chond} = 140 \times 10^{-6}$ and $\alpha = 0.9$, is indicated by a red cross in the panel at the left bottom.

addition of nebula-like hydrogen to the early Earth or a different process for isotopic fractionation of hydrogen inside the early Earth. There is one combination for which we cannot find a satisfactory solution: $\alpha = 0.95$ and $(D/H)_{chond} = 130 \times 10^{-6}$.

Only negligible differences exist between the cases of perfect core mergers and those where the cores perfectly equilibrate with the growing proto-Earth's mantle before they are incorporated into its core (cf. Tables 1 and 2). Using Δ to denote the absolute difference in each of the best fits between the two scenarios, we find $\Delta M_{chond} \leq 0.7$ oceans, $\Delta M_{ingas} \leq 0.02$ oceans, $\Delta M_{core} \leq 0.27$ oceans, and $\Delta(D/H)_{core} \leq 1.1 \times 10^{-6}$. The largest

Table 1
Best Fit Solutions for All Combinations of α and $(D/H)_{chond}$, for the Case of Perfect Core Mergers

$(D/H)_{chond}$	$\alpha = 0.75$	$\alpha = 0.85$	$\alpha = 0.95$
130×10^{-6}	$M_{chond} = 7.20$	$M_{chond} = 8.00$	M_{chond} = n/a
	$M_{ingas} = 0.20$	$M_{ingas} = 0.08$	M_{ingas} = n/a
	$M_{core} = 4.62$	$M_{core} = 4.90$	M_{core} = n/a
	$(D/H)_{core} = 114$	$(D/H)_{core} = 121$	$(D/H)_{core}$ = n/a
	$M_{mantle} = 2.88$	$M_{mantle} = 3.18$	M_{mantle} = n/a
	$(D/H)_{mantle} = 150$	$(D/H)_{mantle} = 149$	$(D/H)_{mantle}$ = n/a
	$\chi^2 = 0.03$	$\chi^2 = 0.39$	$\chi^2 = 7.50$
140×10^{-6}	$M_{chond} = 7.60$	**$M_{chond} = 7.90$**	$M_{chond} = 8.40$
	$M_{ingas} = 0.28$	**$M_{ingas} = 0.14$**	$M_{ingas} = 0.00$
	$M_{core} = 4.75$	**$M_{core} = 4.83$**	$M_{core} = 5.06$
	$(D/H)_{core} = 123$	**$(D/H)_{core} = 130$**	$(D/H)_{core} = 137$
	$M_{mantle} = 3.13$	**$M_{mantle} = 3.18$**	$M_{mantle} = 3.34$
	$(D/H)_{mantle} = 150$	**$(D/H)_{mantle} = 150$**	$(D/H)_{mantle} = 151$
	$\chi^2 = 0.02$	**$\chi^2 = 0.04$**	$\chi^2 = 0.25$
150×10^{-6}	$M_{chond} = 7.40$	$M_{chond} = 7.80$	$M_{chond} = 7.70$
	$M_{ingas} = 0.34$	$M_{ingas} = 0.20$	$M_{ingas} = 0.06$
	$M_{core} = 4.67$	$M_{core} = 4.83$	$M_{core} = 4.79$
	$(D/H)_{core} = 132$	$(D/H)_{core} = 140$	$(D/H)_{core} = 147$
	$M_{mantle} = 3.07$	$M_{mantle} = 3.17$	$M_{mantle} = 2.79$
	$(D/H)_{mantle} = 150$	$(D/H)_{mantle} = 150$	$(D/H)_{mantle} = 150$
	$\chi^2 = 0.01$	$\chi^2 = 0.03$	$\chi^2 = 0.00$
160×10^{-6}	$M_{chond} = 7.30$	$M_{chond} = 7.30$	$M_{chond} = 7.90$
	$M_{ingas} = 0.40$	$M_{ingas} = 0.24$	$M_{ingas} = 0.12$
	$M_{core} = 4.62$	$M_{core} = 4.62$	$M_{core} = 4.86$
	$(D/H)_{core} = 141$	$(D/H)_{core} = 149$	$(D/H)_{core} = 157$
	$M_{mantle} = 3.08$	$M_{mantle} = 2.92$	$M_{mantle} = 3.16$
	$(D/H)_{mantle} = 150$	$(D/H)_{mantle} = 150$	$(D/H)_{mantle} = 150$
	$\chi^2 = 0.01$	$\chi^2 = 0.01$	$\chi^2 = 0.03$
170×10^{-6}	$M_{chond} = 7.00$	$M_{chond} = 7.40$	$M_{chond} = 7.50$
	$M_{ingas} = 0.44$	$M_{ingas} = 0.30$	$M_{ingas} = 0.16$
	$M_{core} = 4.50$	$M_{core} = 4.67$	$M_{core} = 4.71$
	$(D/H)_{core} = 150$	$(D/H)_{core} = 159$	$(D/H)_{core} = 166$
	$M_{mantle} = 2.94$	$M_{mantle} = 3.03$	$M_{mantle} = 2.95$
	$(D/H)_{mantle} = 150$	$(D/H)_{mantle} = 150$	$(D/H)_{mantle} = 150$
	$\chi^2 = 0.06$	$\chi^2 = 0.03$	$\chi^2 = 0.01$

Note. Values of M_{chond} and M_{ingas} that best match M_{mantle} = 3 oceans and $(D/H)_{mantle} = 150 \times 10^{-6}$ are listed for each combination. Masses are expressed in equivalent oceans of hydrogen and D/H ratios in units of 10^{-6}. Likely results for the most plausible combination of α and $(D/H)_{chond}$ are highlighted in bold. *n/a* indicates no solution.

differences occur when $\alpha = 0.95$. We also test an intermediate condition where metal-silicate equilibration between embryo cores and proto-Earth mantle ceases when the mass of the latter reaches 60% of its final value (i.e., $q = 0.6$), as proposed by Rubie et al. (2011), and obtain results falling between those of the end-member scenarios.

Based on the discussion above, we favor an intermediate case with $(D/H)_{chond} \approx 140 \times 10^{-6}$ and $\alpha \approx 0.9$. In this case, Earth would have accreted about seven oceans' worth of hydrogen from chondritic materials and ingassed ~0.06 oceans, a result that agrees well with the outcome of mixing modeling as a different approach (Sarafian et al., 2017). In this favored case, the core would contain about 4.5 oceans' worth of hydrogen, with $D/H \approx 135 \times 10^{-6}$ ($\delta D \approx -133‰$), and the mantle and surface combined would contain about 2.6 oceans of hydrogen, with $D/H \approx 150 \times 10^{-6}$.

5. Discussion

The amount and D/H ratio of hydrogen in Earth's mantle are well matched by models that involve most of Earth's hydrogen deriving from about seven to eight oceans of chondritic water with $(D/H)_{chond} \approx 130$–$170 \times 10^{-6}$, with up to 0.5 oceans from ingassed solar nebula hydrogen with $D/H = 21 \times 10^{-6}$. The most likely input parameters are $(D/H)_{chond} = 140 \times 10^{-6}$ and $\alpha \approx 0.9$, which yield solutions with $M_{chond} \approx 7$ oceans and

Table 2
Same as Table 1 but for the Case of Perfect Equilibration of Cores With the Mantle During Mergers

$(D/H)_{chond}$	$\alpha = 0.75$	$\alpha = 0.85$	$\alpha = 0.95$
130×10^{-6}	$M_{chond} = 7.50$	$M_{chond} = 7.90$	M_{chond} = n/a
	$M_{ingas} = 0.22$	$M_{ingas} = 0.08$	M_{ingas} = n/a
	$M_{core} = 4.71$	$M_{core} = 4.86$	M_{core} = n/a
	$(D/H)_{core} = 115$	$(D/H)_{core} = 122$	$(D/H)_{core}$ = n/a
	$M_{mantle} = 3.01$	$M_{mantle} = 3.12$	M_{mantle} = n/a
	$(D/H)_{mantle} = 150$	$(D/H)_{mantle} = 149$	$(D/H)_{mantle}$ = n/a
	$\chi^2 = 0.01$	$\chi^2 = 0.17$	$\chi^2 = 18.12$
140×10^{-6}	$M_{chond} = 7.30$	**$M_{chond} = 7.80$**	$M_{chond} = 7.70$
	$M_{ingas} = 0.28$	**$M_{ingas} = 0.14$**	$M_{ingas} = 0.00$
	$M_{core} = 4.62$	**$M_{core} = 4.83$**	$M_{core} = 4.79$
	$(D/H)_{core} = 123$	**$(D/H)_{core} = 131$**	$(D/H)_{core} = 138$
	$M_{mantle} = 2.96$	**$M_{mantle} = 3.11$**	$M_{mantle} = 2.91$
	$(D/H)_{mantle} = 150$	**$(D/H)_{mantle} = 150$**	$(D/H)_{mantle} = 150$
	$\chi^2 = 0.03$	**$\chi^2 = 0.01$**	$\chi^2 = 0.02$
150×10^{-6}	$M_{chond} = 7.50$	$M_{chond} = 7.70$	$M_{chond} = 7.20$
	$M_{ingas} = 0.36$	$M_{ingas} = 0.20$	$M_{ingas} = 0.06$
	$M_{core} = 4.71$	$M_{core} = 4.79$	$M_{core} = 4.98$
	$(D/H)_{core} = 131$	$(D/H)_{core} = 140$	$(D/H)_{core} = 147$
	$M_{mantle} = 3.15$	$M_{mantle} = 3.11$	$M_{mantle} = 3.28$
	$(D/H)_{mantle} = 150$	$(D/H)_{mantle} = 150$	$(D/H)_{mantle} = 150$
	$\chi^2 = 0.03$	$\chi^2 = 0.01$	$\chi^2 = 0.15$
160×10^{-6}	$M_{chond} = 7.10$	$M_{chond} = 7.30$	$M_{chond} = 7.50$
	$M_{ingas} = 0.40$	$M_{ingas} = 0.24$	$M_{ingas} = 0.10$
	$M_{core} = 4.54$	$M_{core} = 4.62$	$M_{core} = 4.71$
	$(D/H)_{core} = 140$	$(D/H)_{core} = 149$	$(D/H)_{core} = 157$
	$M_{mantle} = 2.96$	$M_{mantle} = 2.92$	$M_{mantle} = 2.89$
	$(D/H)_{mantle} = 150$	$(D/H)_{mantle} = 150$	$(D/H)_{mantle} = 150$
	$\chi^2 = 0.01$	$\chi^2 = 0.04$	$\chi^2 = 0.01$
170×10^{-6}	$M_{chond} = 7.10$	$M_{chond} = 7.30$	$M_{chond} = 7.70$
	$M_{ingas} = 0.46$	$M_{ingas} = 0.30$	$M_{ingas} = 0.16$
	$M_{core} = 4.54$	$M_{core} = 4.62$	$M_{core} = 4.79$
	$(D/H)_{core} = 149$	$(D/H)_{core} = 158$	$(D/H)_{core} = 166$
	$M_{mantle} = 3.02$	$M_{mantle} = 2.98$	$M_{mantle} = 3.07$
	$(D/H)_{mantle} = 150$	$(D/H)_{mantle} = 150$	$(D/H)_{mantle} = 150$
	$\chi^2 = 0.01$	$\chi^2 = 0.02$	$\chi^2 = 0.03$

$M_{ingas} \approx 0.06$ oceans, for which about 4.5 oceans' worth of hydrogen with $(D/H) = 135 \times 10^{-6}$ would be sequestered in the core. If seven to eight oceans of water were accreted from chondrites, it is likely that the majority of this water was from carbonaceous chondrites, as ordinary chondrites would likely supply only about 0.3 oceans of water. This distribution justifies the range of $(D/H)_{chond}$ we have considered, which are appropriate for carbonaceous chondrites but not ordinary chondrites.

The amount and D/H of hydrogen that we predict is stored in Earth's core is based on our estimates of hydrogen solubility at high pressures and its isotope fractionation into iron using low-pressure proxies. The model would benefit greatly from direct measurement of these parameters. Even though our results carry uncertainties with no doubt, the current model offers better constraints than previous studies (e.g., Genda, 2016, and references therein) on both elemental abundances and isotopic compositions of hydrogen in Earth's major reservoirs.

Although we find that most (~60%) of Earth's hydrogen resides in its core, the effect of that hydrogen on the core density is small. With four to five oceans of hydrogen dissolved, the core has a hydrogen mass concentration ranging between 0.034 and 0.043 wt %, equivalent to a molar ratio Fe:H ≈ 1:0.02, which would reduce the core density by possibly 0.27%, only a small fraction of the observed total deficit.

5.1. Sensitivity of Results to Hydrogen Solubility in Metals

The amount of hydrogen that enters the core is proportional to the solubility of hydrogen in iron, according to the model. That is, to say, a 10% difference in the solubility would translate into a 10% difference in the

hydrogen content in the core. Direct application of c_H calculated above to Earth's core may cause deviation from the reality because of at least two reasons—(1) uncertainties of thermodynamic parameters used in the model and (2) effect of carbon on hydrogen solubility.

Our results are predicated on the use of Sievert's law to calculate the solubility of hydrogen in liquid iron at a typical range of effective hydrogen pressures ($P_{H_2} \approx$ 1–10 MPa) and two specific temperatures (T = 2500 and 3500 K), using $\Delta H°$ and $\Delta S°$ reported by Fromm and Hörz (1980). When assessing these uncertainties, we care about the lower limit of cH_2 more than the upper limit, because elevated cH_2 would lead to increased M_{core} and thus even reinforce our conclusion. In this regard, variations of 10% in P_{H_2}, T, $\Delta H°$, and $\Delta S°$ yield variations in cH_2 of ~5%, ~11%, ~10%, and ~37%, respectively. From these numbers we see that the largest uncertainty would come from the thermodynamic measurements for hydrogen dissolution in liquid iron, which are probably the most constrained among these modeling inputs because they are from experimental measurements. If we permute and combine the 10% variations of all these parameters, the propagated variation would be <53%, use of which in the model would yield $M_{core} > 2.3$ oceans and $M_{ingas} > 0.02$ oceans for the most plausible case. Such a factor-of-2 variation in M_{core} would not refute our general conclusion that a substantial amount of hydrogen comparable to the mantle content exists in the core and a nonzero component of ingassed hydrogen is invoked to satisfy the isotopic constraints. Hence, the model is not altered by ~10% variations in these thermodynamic inputs.

Recent experiments by Clesi et al. (2018) indicate that the hydrogen solubility could be significantly lower than our assumed values. They suggest partition coefficients of hydrogen into liquid iron, D_H, lower than what we assume by an order of magnitude, suggesting hydrogen concentrations in planetary cores are <60 ppm. A similar result would be found if their D_H are used in our model; however, we notice that the goodness-of-fit parameter χ^2 is always >3.5. In other words, the present model has no solutions unless the real partition coefficients are significantly greater than theirs. In fact, seeing that their experiments allowed substantial carbon in the iron melt, we believe that their results indicate a sensitivity of hydrogen solubility to carbon content that can be accounted for.

Several factors suggest that carbon played a role in Clesi et al. (2018) measurements. Their experimental design used (inner) graphite capsules and temperatures above 2000 K, providing an opportunity for iron in their samples to be saturated with carbon. This situation is in contrast to previous experiments that used no graphite and found higher solubilities (Okuchi, 1997; Shibazaki et al., 2009). In addition, Clesi et al. (2018) inferred carbon concentrations of 3 to 7 wt %, a significant fraction of the saturation concentration of carbon, 6.67 wt %, as in Fe_3C. Actually, Clesi et al. (2018) did not measure carbon directly, instead calculating it as the balance after all other elements were accounted for, so it is possible that the carbon concentrations were even closer to saturation than their estimates. Percent-level concentrations of carbon would likely decrease D_H appreciably, possibly owing to the limiting effect of carbon on hydrogen solubility in iron, which has been experimentally confirmed both in Fe-C melts at 1865 K and 1 bar (Weinstein & Elliott, 1963) and in carbon steels at 500–900 K and 0.1–7 bar (Gadgeel & Johnson, 1979).

If the low solubility of hydrogen in the experiments of Clesi et al. (2018) is attributable to the carbon content, it is possible to account for this effect. Both theoretical and experimental analyses have demonstrated that the logarithm of the partition coefficient, $\log_{10}D_H$, is linearly proportional to the inverse of temperature, and to the abundance of incompatible elements, in many geological solution systems (McIntire, 1963). The partition coefficients reported by Clesi et al. (2018) for two iron specimens at ~20 GPa and ~2735 K with carbon concentrations of 7.50 and 5.44 wt % (whose average is close to the 6.67 wt % of Fe_3C), can be taken as an approximation of D_H between carbon-saturated iron liquid and silicate melt. These numbers yield $D_H \approx 0.56$. For the partition coefficient between carbon-free iron and silicate, we take the value that we calculate using Sieverts' law, deriving $D_H > 4.73$, a result consistent with the experimental results of Okuchi (1997) and Shibazaki et al. (2009). Interpolating between these extremes, we then obtain $\log_{10}D_H = 0.675–0.925\cdot(f_C/6.67$ wt %), where f_C is the mass fraction of carbon in the iron. Earth's core has $f_C < 1$ wt % (Wood et al., 2013), possibly <0.25 wt % (Dasgupta & Walker, 2008), suggesting that our partition coefficient assuming carbon-free iron is overestimated by no more than 27%, perhaps only 8%.

Use of the approximations above yields $D_H > 3.44$ at 20 GPa and 2735 K for $f_C < 1$ wt %, and application of the $\log_{10}D_H - 1/T$ relation (Okuchi, 1997) gives lower limits of D_H at 20 GPa and different temperatures. Finally,

input of appropriate D_H values into our model produces results that take carbon effects into account and differ from those of corresponding carbon-free cases to limited extents. When $\alpha = 0.85$, for example, (ΔM_{chond}, ΔM_{ingas}) = (−2.4 oceans, −0.08 oceans), (−1.4 oceans, −0.08 oceans), (−1.6 oceans, −0.04 oceans), (−1.2 oceans, +0.02 oceans), and (−1.2 oceans, +0.06 oceans) for $(D/H)_{chond} = 130 \times 10^{-6}$, 140×10^{-6}, 150×10^{-6}, 160×10^{-6}, and 170×10^{-6}, respectively, in the case of $q = 0.6$. These Δ values would further diminish when the actual D_H is used and/or if a smaller carbon abundance than 1 wt % exists in the core. The results here confirm that the effects of <1 wt % carbon in the core would be to reduce hydrogen content by <30%. On the contrary, because of the positive effect of nickel on hydrogen solubility (Busch & Dodd, 1960), alloying of ~5 wt % nickel to iron in the core would probably increase the hydrogen content.

5.2. Low-D/H Material Near Earth's Core-Mantle Boundary

Beyond the effects relevant to the core, our model predicts the presence of low-D/H material at the core-mantle boundary. Picrite inclusions from Baffin Island and Icelandic lavas, associated with high $^3He/^4He$ ratios and a reported mantle-plume origin, have $D/H \leq 122 \times 10^{-6}$ and have been interpreted to come from a primitive, volatile-rich reservoir that originated from near the core-mantle boundary (Hallis et al., 2015). They attributed this isotopically light hydrogen either to a source inherited directly from the solar nebula, such as isotopically light H_2O adsorbed directly onto dust grains (Drake, 2005), or to solar wind hydrogen that may have been implanted into accreting materials. Hallis et al. (2015) also suggested that top-down crystallization of a magma ocean would have trapped volatile elements in cumulates at the deepest mantle.

Our model explains the existence of a heterogeneous, low-D/H reservoir of hydrogen near the core-mantle boundary as the result of ingassing. As soon as a magma ocean developed at the surface of proto-Earth, dissolution of a nebula-captured, hydrogen-rich protoatmosphere into the magma was inevitable. Once the magma ocean started to crystallize, partitioning of volatiles including hydrogen occurred between solid cumulates, evolving liquids, and a growing protoatmosphere (Elkins-Tanton, 2008). Overturn of the heavy cumulates would have trapped the D-depleted hydrogen, likely owing to inefficient melt drainage out of the freezing front of a crystallizing magma ocean (Hier-Majumder & Hirschmann, 2017), and transported it to as deep as the core-mantle boundary. Some of these cumulates probably remixed with the mantle over time, but the mixing was almost certainly incomplete.

It is possible that the above-mentioned deepest, densest material comprises some or most of the LLSVPs or especially ULVZs. The latter are likely associated with Fe-rich silicates (Mao et al., 2006). Our calculations suggest that if this material formed by crystallization of a surface (not basal) magma ocean with ingassed solar nebula hydrogen, it could be as isotopically light as $D/H \approx 109 \times 10^{-6}$. Alternatively, ULVZs may have formed by reaction between the lower mantle and core, with attendant isotopic exchange of hydrogen between them. In that case, materials in the lower mantle might have acquired a D/H ratio as low as 120×10^{-6} ($\delta D = -230‰$), albeit only for cases with low α and low $(D/H)_{chond} \approx 130 \times 10^{-6}$.

Tighter constraints on the D/H ratio in materials transported from the deep mantle by plumes may therefore test the ingassing hypothesis and whether ULVZs formed by magma ocean overturn or by isotopic exchange with the core.

5.3. Earth's Inventory of Solar Neon and Helium

Our model also makes testable predictions about Earth's inventory of noble gases. Subject to the assumed value of α, a robust result of our model is that Earth likely ingassed ~0.1 ocean's worth of hydrogen from a protoatmosphere accreted from the solar nebula. Some of the noble gases in Earth, particularly ^3He and ^{22}Ne, are widely assumed to have derived from the solar nebula (Mizuno et al., 1980; Mottl et al., 2007). We therefore examine whether the terrestrial inventories of these gases would have ingassed together with the expected amount of hydrogen. We take 0.1 oceans' worth of hydrogen, or 8.5×10^{21} moles of H_2, as typical.

We assume a hydrogen pressure $P_{H_2} \approx 1$ bar, an approximate value for a protoatmosphere around a 0.4-M_E embryo (Stökl et al., 2015, Figure 10). For hydrogen in contact with a magma ocean of the expected redox condition, P_{H_2O}/P_{H_2} in the protoatmosphere was between ~0.01 and 0.1. The water fraction in the atmosphere increased with increasing oxidation: for example, at 1500 K and the IW buffer, $P_{H_2O}/P_{H_2} = 0.88$ (Ikoma & Genda, 2006). The mass fraction of H_2O dissolved in the magma ocean was $x_{H_2O} = 300 \cdot (P_{H_2O}/0.1\ bar)^{1/2}$ ppm (Fricker &

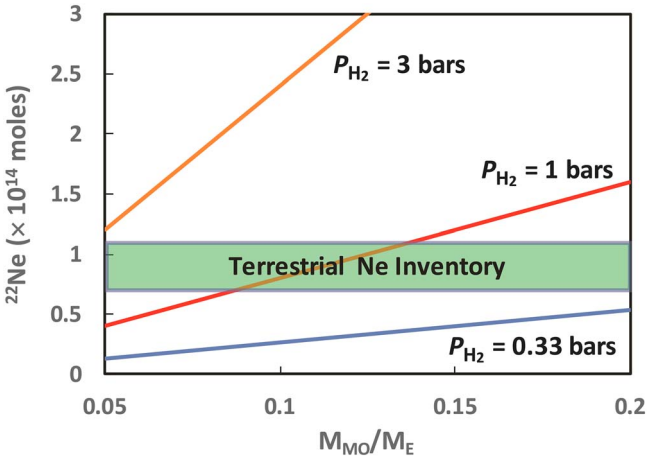

Figure 3. The ingassed neon inventory as a function of the mass of equilibrated magma ocean and pressure of nebula-originated protoatmosphere. For protoatmospheric pressures and magma ocean masses characteristic of planetary embryos, the modern terrestrial *solar* neon inventory could have been ingassed via equilibrium dissolution. Similar considerations apply to primordial ^{3}He (see section 5.3).

Reynolds, 1968; Moore et al., 1998), and the mass fraction of dissolved H_2 was $x_{H_2} = 0.1 \cdot (P_{H_2}/1\ \text{bar})$ ppm (Hirschmann et al., 2012), so even though H_2 would have been the dominant form of atmospheric hydrogen, it essentially dissolved into the magma ocean only as H_2O (more precisely, as OH). Assuming a 1-bar atmosphere, if $P_{H_2O}/P_{H_2} = 0.1$, then $P_{H_2O} = 0.1$ bar and the mass fraction $x_{H_2O} = 300$ ppm is equivalent to dissolving 0.06 oceans of hydrogen into a 0.05-M_E magma ocean. If $P_{H_2O}/P_{H_2} = 0.01$, then $P_{H_2O} = 0.01$ bar and the mass fraction $x_{H_2O} = 94$ ppm is equivalent to dissolving 0.06 oceans of hydrogen into a 0.16-M_E magma ocean. These magma ocean masses are consistent with those produced during the energetic embryo-embryo collisions that are thought necessary to create ~0.4-M_E planetary objects (Abe, 1997).

Earth's atmosphere has ^{20}Ne/^{22}Ne = 9.8, implying a mixture of ~65% ^{22}Ne from accreted, chondritic neon with ^{20}Ne/^{22}Ne = 8.5, and ~35% ^{22}Ne from ingassed, solar nebula neon with ^{20}Ne/^{22}Ne = 13.5 (Jaupart et al., 2017; Lodders, 2003). Based on the molar abundance ~1.82×10^{-5} of Ne in Earth's atmosphere, which has a mass of 5.15×10^{18} kg, this distribution implies that 1.1×10^{14} moles of ^{22}Ne were ingassed. Likewise, the inferred abundance of ^{22}Ne in the deep mantle is 1.9×10^{-14} mol/g (Yokochi & Marty, 2004) which, if considered as an average primitive-mantle concentration, yields 7.6×10^{13} moles of ^{22}Ne. We infer that ~10^{14} moles of ^{22}Ne must be ingassed. A similar amount of ^{3}He also must be ingassed. Unlike Ne, ^{3}He was thermally lost from Earth's atmosphere on approximately million-year timescales, so its inventory must be constrained entirely from deep sources. Typical values of ^{3}He/^{22}Ne in the deep Earth, for example, in the Hawaii plume, are ~6 (Honda & McDougall, 1998), yielding 6×10^{14} moles of terrestrial ^{3}He. A test of the ingassing hypothesis is whether this much ^{3}He and ^{22}Ne would be ingassed alongside the predicted ingassed hydrogen.

In a protoatmosphere of solar composition with $P_{H_2} = 1$ bar, the partial pressure of ^{22}Ne would have been 1.2×10^{-5} bar (Lodders, 2003). The neon solubility into a basaltic melt is 25×10^{-5} cc/(g·bar) (Jambon et al., 1986), from which we derive a mass fraction of ^{22}Ne in the magma ocean of 2.9×10^{-12}, which in a 0.05–0.20-M_E magma ocean yields $0.4–1.6 \times 10^{14}$ moles of ^{22}Ne. Likewise, the pre-D burning ^{3}He/^{4}He of the solar nebula—inferred from the Jovian atmosphere—is 1.7×10^{-4} (Lodders, 2003), yielding a partial pressure for ^{3}He of 3.2×10^{-5} bars in a 1-bar solar composition (H_2-dominated) atmosphere. The solubility of He in basaltic melts is 56×10^{-5} cc/(g·bar) (Jambon et al., 1986), from which we derive a magmatic ^{3}He mass fraction of 2.4×10^{-12}. In a 0.05- to 0.20-M_E magma ocean this mass fraction yields $2.4–9.6 \times 10^{14}$ moles of dissolved ^{3}He. More ^{3}He and ^{22}Ne could have been ingassed if the protoatmosphere was more massive, the magma ocean was larger, more chemically reduced, or a combination of these factors.

The terrestrial inventories of both ^{3}He and ^{22}Ne therefore can be explained by ingassing into a magma ocean from the nebula-originated protoatmosphere. The effective solubility of hydrogen (as H_2O rather than H_2) is consistent with ingassing of 0.1 oceans' worth of hydrogen from a 1-bar, solar composition protoatmosphere into magma oceans of mass 0.20–0.05 M_E, for atmospheric $P_{H_2O}/P_{H_2} = 0.01–0.1$, consistent with redox conditions between IW-4 and IW-2. The masses of ^{22}Ne and ^{3}He that would dissolve into the magma ocean under these conditions are quantitatively consistent with the known terrestrial inventories of these gases (Figure 3).

6. Conclusions

Our comprehensive model for the origin of Earth's water considers, for the first time, the effects of isotopic fractionation as hydrogen dissolved into metal and was sequestered into the core. Based on the behaviors of proxies, we consider it likely that the D/H ratio of the core is ~10% lighter than the mantle. We hypothesize that Earth accreted a few to tens of oceans of water from chondrites, mostly carbonaceous chondrites. Drawing on the latest theories of planet formation, which argue for rapid (<2 Myr) formation of planetary embryos, we favor ingassing of a few tenths of an ocean of solar nebula hydrogen into the magma oceans of the embryos that formed Earth.

Based on modeling, we favor scenarios in which chondrites contributed seven to eight oceans of hydrogen, and about 0.06 oceans of hydrogen was ingassed, unless Earth's core contains a significant amount of carbon (>1 wt %). Such models are consistent with about four to five oceans of hydrogen sequestered in the core, with D/H possibly as low as 120×10^{-6}, and approximately three oceans of hydrogen in the mantle and surface, with D/H = 150×10^{-6}.

The predicted existence of majority of Earth's hydrogen in its core has only a minor contribution to the observed density deficit of the core, a result consistent with the current knowledge of light elements in the core. Our conclusions are not overly sensitive to reasonable uncertainties in thermodynamic quantities governing hydrogen solubility in iron. We interpret the anomalously low solubilities measured by Clesi et al. (2018) to reflect the effect of carbon. Accounting for this effect and assuming <1 wt % carbon in Earth's core, we find not large differences compared to the case presented here.

Both ingassing of isotopically light hydrogen and isotopic fractionation of hydrogen as it is sequestered into the core provide an explanation for the low-D/H material sampled by Hallis et al. (2015). Either the measurements are of solidified magma ocean material containing ingassed solar nebula hydrogen or they are of lower mantle material that has isotopically exchanged with the core. Testing our model and distinguishing between these scenarios will require the technically challenging measurements of the solubility of hydrogen into iron, and the isotopic fractionation factor, α, at high pressures. Firmer constraints on the bulk D/H ratios of various chondrites would also constrain the model.

Our model explains the reported solar compositions of hydrogen and noble gases in Earth's mantle. In particular, nebular ingassing through equilibration dissolution appears to be a viable mechanism to supply adequate amounts of ^{22}Ne and ^{3}He for their terrestrial inventories, provided that the mass of magma ocean was no less than ~0.1 M_E. Extension to other noble gases would further test the model.

Acknowledgments
This work was mainly supported by the research grant "Water from the Heavens: The Origins of Earth's Hydrogen" sponsored by the W. M. Keck Foundation (P.I. Peter Buseck). The results benefited from collaborations and/or information exchange within NASA's Nexus for Exoplanet System Science (NExSS) research coordination network sponsored by NASA's Science Mission Directorate (grant NNX15AD53G and P.I. Steven Desch). We thank Adam Sarafian and an anonymous reviewer for their constructive comments and suggestions on an earlier manuscript. All the data sets required to create the figures and tables in this work can be generated using the FORTRAN codes that are included in the supporting information.

References

Abe, Y. (1997). Thermal and chemical evolution of the terrestrial magma ocean. *Physics of the Earth and Planetary Interiors*, *100*(1-4), 27–39. https://doi.org/10.1016/S0031-9201(96)03229-3

Albarede, F., Ballhaus, C., Blichert-Toft, J., Lee, C.-T., Marty, B., Moynier, F., & et al. (2013). Asteroid impacts and the origin of terrestrial and lunar volatiles. *Icarus*, *222*(1), 44–52. https://doi.org/10.1016/j.icarus.2012.10.026

Alexander, C. M. O.'. D. (2017). The origin of inner solar system water. *Philosophical Transactions of the Royal Society A*, *375*, 20150384. https://doi.org/10.1098/rsta.2015.0384

Alexander, C. M. O.'. D., Barber, D. J., & Hutchison, R. (1989). The microstructure of Semarkona and Bishunpur. *Geochimica et Cosmochimica Acta*, *53*(11), 3045–3057. https://doi.org/10.1016/0016-7037(89)90180-4

Alexander, C. M. O.'. D., Bowden, R., Fogel, M. L., Howard, K. T., Herd, C. D. K., & Nittler, L. R. (2012). The provenances of asteroids, and their contributions to the volatile inventories of the terrestrial planets. *Science*, *337*(6095), 721–723. https://doi.org/10.1126/science.1223474

Alexander, C. M. O.'. D., Howard, K. T., Bowden, R., & Fogel, M. L. (2013). The classification of CM and CR chondrites using bulk H, C and N abundances and isotopic compositions. *Geochimica et Cosmochimica Acta*, *123*, 244–260. https://doi.org/10.1016/j.gca.2013.05.019

Altwegg, K., Balsiger, H., Bar-Nun, A., Berthelier, J. J., Bieler, A., Bochsler, P., et al. (2015). 67P/Churyumov-Gerasimenko, a Jupiter family comet with a high D/H ratio. *Science*, *347*(6220), 1261952. https://doi.org/10.1126/science.1261952

Andreev, B. M., & Magomedbekov, E. P. (2001). Separation of hydrogen isotopes by chemical isotope exchange in systems involving metal and intermetallic compound hydrides. *Separation Science and Technology*, *36*(8-9), 2027–2086. https://doi.org/10.1081/SS-100104766

Badro, J., Côté, A. S., & Brodholt, J. P. (2014). A seismologically consistent compositional model of Earth's core. *Proceedings of the National Academy of Sciences of the United States of America*, *111*(21), 7542–7545. https://doi.org/10.1073/pnas.1316708111

Bercovici, D., & Karato, S.-I. (2003). Whole-mantle convection and the transition-zone water filter. *Nature*, *425*(6953), 39–44. https://doi.org/10.1038/nature01918

Birch, F. (1952). Elasticity and constitution of the Earth's interior. *Journal of Geophysical Research*, *57*(2), 227–286. https://doi.org/10.1029/JZ057i002p00227

Bottke, W. F., Nesvorný, D., Vokrouhlický, D., & Morbidelli, A. (2010). The irregular satellites: The most collisionally evolved populations in the solar system. *Astronomy Journal*, *139*(3), 994–1014. https://doi.org/10.1088/0004-6256/139/3/994

Brauer, F., Dullemond, C. P., & Henning, T. (2008). Coagulation, fragmentation and radial motion of solid particles in protoplanetary disks. *Astronomy and Astrophysics*, *480*(3), 859–877. https://doi.org/10.1051/0004-6361:20077759

Brown, S. M., Elkins-Tanton, L. T., & Walker, R. J. (2014). Effects of magma ocean crystallization and overturn on the development of ^{142}Nd and ^{182}W isotopic heterogeneities in the primordial mantle. *Earth and Planetary Science Letters*, *408*, 319–330. https://doi.org/10.1016/j.epsl.2014.10.025

Busch, T., & Dodd, R. A. (1960). The solubility of hydrogen and nitrogen in liquid alloys of iron, nickel, and cobalt. *Transactions of the Metallurgical Society of the American Institute of Mechanical Engineers*, *218*, 488–490.

Caracas, R. (2015). The influence of hydrogen on the seismic properties of solid iron. *Geophysical Research Letters*, *42*, 3780–3785. https://doi.org/10.1002/2015GL063478

Clesi, V., Bouhifd, M. A., Bolfan-Casanova, N., Manthilake, G., Schiavi, F., Raepsaet, C., et al. (2018). Low hydrogen contents in the cores of terrestrial planets. *Science Advances*, *4*(3), e1701876. https://doi.org/10.1126/sciadv.1701876

Clog, M., Aubaud, C., Cartigny, P., & Dosso, L. (2013). The hydrogen isotopic composition and water content of southern Pacific MORB: A reassessment of the D/H ratio of the depleted mantle reservoir. *Earth and Planetary Science Letters*, *381*, 156–165. https://doi.org/10.1016/j.epsl.2013.08.043

Dahl, T. W., & Stevenson, D. J. (2010). Turbulent mixing of metal and silicate during planet accretion—And interpretation of the Hf-W chronometer. *Earth and Planetary Science Letters*, *295*(1-2), 177–186. https://doi.org/10.1016/j.epsl.2010.03.038

Dalou, C., Le Losq, C., & Mysen, B. O. (2015). In situ study of the fractionation of hydrogen isotopes between aluminosilicate melts and coexisting aqueous fluids at high pressure and high temperature—Implications for the δD in magmatic processes. *Earth and Planetary Science Letters*, *426*, 158–166. https://doi.org/10.1016/j.epsl.2015.06.032

Dasgupta, R., & Walker, D. (2008). Carbon solubility in core melts in a shallow magma ocean environment and distribution of carbon between the Earth's core and the mantle. *Geochimica et Cosmochimica Acta*, *72*(18), 4627–4641. https://doi.org/10.1016/j.gca.2008.06.023

Dauphas, N. (2017). The isotopic nature of the Earth's accreting material through time. *Nature*, *541*(7638), 521–524. https://doi.org/10.1038/nature20830

Dauphas, N., Chen, J. H., Zhang, J., Papanastassiou, D. A., Davis, A. M., & Travaglio, C. (2014). Calcium-48 isotopic anomalies in bulk chondrites and achondrites: Evidence for a uniform isotopic reservoir in the inner protoplanetary disk. *Earth and Planetary Science Letters*, *407*, 96–108 . https://doi.org/10.1016/j.epsl.2014.09.015

Dauphas, N., & Pourmand, A. (2011). Hf-W-Th evidence for rapid growth of Mars and its status as a planetary embryo. *Nature*, *473*(7348), 489–492. https://doi.org/10.1038/nature10077

Drake, M. J. (2005). Origin of water in the terrestrial planets. *Meteoritics and Planetary Science*, *40*, 1–9.

Drake, M. J., & Righter, K. (2002). Determining the composition of the Earth. *Nature*, *416*(6876), 39–44. https://doi.org/10.1038/416039a

Elkins-Tanton, L. T. (2008). Linked magma ocean solidification and atmospheric growth for Earth and Mars. *Earth and Planetary Science Letters*, *271*(1-4), 181–191. https://doi.org/10.1016/j.epsl.2008.03.062

Elkins-Tanton, L. T. (2011). Formation of early water oceans on rocky planets. *Astrophysics and Space Science*, *332*(2), 359–364. https://doi.org/10.1007/s10509-010-0535-3

Elkins-Tanton, L. T. (2012). Magma oceans in the inner solar system. *Annual Review of Earth and Planetary Sciences*, *40*(1), 113–139. https://doi.org/10.1146/annurev-earth-042711-105503

Fricker, P. E., & Reynolds, R. T. (1968). Development of the atmosphere of Venus. *Icarus*, *9*(1-3), 221–230. https://doi.org/10.1016/0019-1035(68)90017-1

Fromm, E., & Hörz, G. (1980). Hydrogen, nitrogen, oxygen, and carbon in metals. *International Materials Reviews*, *25*, 269–311.

Fukai, Y. (1984). The iron-water reaction and the evolution of the Earth. *Nature*, *308*(5955), 174–175. https://doi.org/10.1038/308174a0

Fukai, Y. (2005). The structure and phase diagram of M-H systems at high chemical potentials—High pressure and electrochemical synthesis. *Journal of Alloys and Compounds*, *404–406*, 7–15. https://doi.org/10.1016/j.jallcom.2005.02.075

Gadgeel, V. L., & Johnson, D. L. (1979). Gas-phase hydrogen permeation and diffusion in carbon steels as a function of carbon content from 500 to 900 K. *Journal of Materials for Energy Systems*, *1*(2), 32–40. https://doi.org/10.1007/BF02833976

Geiss, J., & Gloeckner, G. (1998). Abundances of deuterium and helium-3 in the protosolar cloud. *Space Science Reviews*, *84*(1/2), 239–250. https://doi.org/10.1023/A:1005039822524

Genda, H. (2016). Origin of Earth's oceans: An assessment of the total amount, history and supply of water. *Geochemical Journal*, *50*(1), 27–42. https://doi.org/10.2343/geochemj.2.0398

Genda, H., Brasser, R., & Mojzsis, S. J. (2017). The terrestrial late veneer from core disruption of a lunar-sized impactor. *Earth and Planetary Science Letters*, *480*, 25–32. https://doi.org/10.1016/j.epsl.2017.09.041

Greenwood, R. C., Barrat, J.-A., Miller, M. F., Anand, M., Dauphas, N., Franchi, I. A., et al. (2018). Oxygen isotopic evidence for accretion of Earth's water before a high-energy Moon-forming giant impact. *Science Advances*, *4*, eaao5928. https://doi.org/10.1126/sciadv.aao5928

Haisch, K. E. Jr., Lada, E. A., & Lada, C. J. (2001). Disk frequencies and lifetimes in young clusters. *The Astrophysical Journal*, *553*(2), L153–L156. https://doi.org/10.1086/320685

Hallis, L. J. (2017). D/H ratios of the inner solar system. *Philosophical Transactions of the Royal Society A*, *375*(2094), 20150390. https://doi.org/10.1098/rsta.2015.0390

Hallis, L. J., Huss, G. R., Nagashima, K., Taylor, G. J., Halldórsson, S. A., Hilton, D. R., et al. (2015). Evidence for primordial water in Earth's deep mantle. *Science*, *350*(6262), 795–797. https://doi.org/10.1126/science.aac4834

Hamano, K., Abe, Y., & Genda, H. (2013). Emergence of two types of terrestrial planet on solidification of magma ocean. *Nature*, *497*(7451), 607–610. https://doi.org/10.1038/nature12163

Harper, C. L. Jr., & Jacobsen, S. B. (1996). Noble gases and Earth's accretion. *Science*, *273*(5283), 1814–1818. https://doi.org/10.1126/science.273.5283.1814

Hartogh, P., Lis, D. C., Bockelée-Morvan, D., de Val-Borro, M., Biver, N., Küppers, M., et al. (2011). Ocean-like water in the Jupiter-family comet 103P/Hartley 2. *Nature*, *478*(7368), 218–220. https://doi.org/10.1038/nature10519

Hawkins, N. J. (1953). *Solubility of hydrogen isotopes in nickel and type 347 stainless steel*. Schenectady, New York: Knolls Atomic Power Laboratory.

Hess, P. C., & Parmentier, E. M. (1995). A model for the thermal and chemical evolution of the Moon's interior: Implications for the onset of mare volcanism. *Earth and Planetary Science Letters*, *134*(3-4), 501–514. https://doi.org/10.1016/0012-821X(95)00138-3

Heumann, T., & Primas, D. (1966). Zum isotopieeffekt der diffusion von wasserstoff und deuterium in reinsteinsen. *Zeitschrift für Naturforschung A*, *21*, 260–265.

Hier-Majumder, S., & Hirschmann, M. M. (2017). The origin of volatiles in the Earth's mantle. *Geochemistry, Geophysics, Geosystems*, *18*, 3078–3092. https://doi.org/10.1002/2017GC006937

Hirose, K., Labrosse, S., & Hernlund, J. (2013). Composition and state of the core. *Annual Review of Earth and Planetary Sciences*, *41*(1), 657–691. https://doi.org/10.1146/annurev-earth-050212-124007

Hirschmann, M. M. (2006). Water, melting, and the deep earth H_2O cycle. *Annual Review of Earth and Planetary Sciences*, *34*(1), 629–653. https://doi.org/10.1146/annurev.earth.34.031405.125211

Hirschmann, M. M. (2012). Magma ocean influence on early atmosphere mass and composition. *Earth and Planetary Science Letters*, *341–344*, 48–57.

Hirschmann, M. M., Withers, A. C., Ardia, P., & Foley, N. T. (2012). Solubility of molecular H in silicate melts and consequences for volatile evolution of terrestrial planets. *Earth and Planetary Science Letters*, *345–348*, 38–48. https://doi.org/10.1016/j.epsl.2012.06.031

Honda, M., & McDougall, I. (1998). Primordial helium and neon in the Earth—A speculation on early degassing. *Geophysical Research Letters*, *25*(11), 1951–1954. https://doi.org/10.1029/98GL01329

Iizuka-Oku, R., Yagi, T., Gotou, H., Okuchi, T., Hattori, T., & Sano-Furukawa, A. (2017). Hydrogenation of iron in the early stage of Earth's evolution. *Nature Communications*, *8*, 14,096. https://doi.org/10.1038/ncomms14096

Ikoma, M., & Genda, H. (2006). Constraints on the mass of a habitable planet with water of nebular origin. *The Astrophysical Journal*, *648*(1), 696–706. https://doi.org/10.1086/505780

Jambon, A., Weber, H., & Braun, O. (1986). Solubility of He, Ne, Ar, Kr and Xe in a basalt melt in the range 1250–1600°C. Geochemical implications. *Geochimica et Cosmochimica Acta*, *50*(3), 401–408. https://doi.org/10.1016/0016-7037(86)90193-6

Jaupart, E., Charnoz, S., & Moreira, M. (2017). Primordial atmosphere incorporation in planetary embryos and the origin of Neon in terrestrial planets. *Icarus*, *293*, 199–205. https://doi.org/10.1016/j.icarus.2017.04.022

Johansen, A., Oishi, J. S., Mac Low, M.-M., Klahr, H., Henning, T., & Youdin, A. (2007). Rapid planetesimal formation in turbulent circumstellar disks. *Nature*, *448*(7157), 1022–1025. https://doi.org/10.1038/nature06086

Kleine, T., Münker, C., Mezger, K., & Palme, H. (2002). Rapid accretion and early core formation on asteroids and the terrestrial planets from Hf-W chronometry. *Nature*, *418*(6901), 952–955. https://doi.org/10.1038/nature00982

Kleine, T., Touboul, M., Bourdon, B., Nimmo, F., Mezger, K., Palme, H., et al. (2009). Hf-W chronology of the accretion and early evolution of asteroids and terrestrial planets. *Geochimica et Cosmochimica Acta*, *73*(17), 5150–5188. https://doi.org/10.1016/j.gca.2008.11.047

Krot, A. N., Nagashima, K., Alexander, C. M. O. D., Ciesla, F. J., Fujiya, W., & Bonal, L. (2015). Sources of water and aqueous activity on the chondrite parent asteroids. In P. Michel, F. E. DeMeo, & W. F. Bottke (Eds.), *Asteroids IV*, *University of Arizona Press*, (pp. 635–660). AZ: Tucson. https://doi.org/10.2458/azu_uapress_9780816532131-ch033

Kruijer, T. S., Burkhardt, C., Budde, G., & Kleine, T. (2017). Age of Jupiter inferred from the distinct genetics and formation times of meteorites. *Proceedings of the National Academy of Sciences of the United States of America*, *114*, 6712–6716. https://doi.org/10.1073/pnas.1704461114

Kuebler, K. E., McSween, H. Y. Jr., Carlson, W. D., & Hirsch, D. (1999). Sizes and masses of chondrules and metal-troilite grains in ordinary chondrites: Possible implications for nebular sorting. *Icarus*, *141*(1), 96–106. https://doi.org/10.1006/icar.1999.6161

Lacher, J. R. (1937). A theoretical formula for the solubility of hydrogen in palladium. *Proceedings of the Royal Society A*, *161*(907), 525–545. https://doi.org/10.1098/rspa.1937.0160

Lambrechts, M., & Johansen, A. (2012). Rapid growth of gas-giant cores by pebble accretion. *Astronomy and Astrophysics*, *544*, A32. https://doi.org/10.1051/0004-6361/201219127

Lécuyer, C., Gillet, P., & Robert, F. (1998). The hydrogen isotope composition of seawater and the global water cycle. *Chemical Geology*, *145*(3-4), 249–261. https://doi.org/10.1016/S0009-2541(97)00146-0

Levison, H. F., Kretke, K. A., Walsh, K. J., & Bottke, W. F. (2015). Growing the terrestrial planets from the gradual accumulation of submeter-sized objects. *Proceedings of the National Academy of Sciences of the United States of America*, *112*(46), 14,180–14,185. https://doi.org/10.1073/pnas.1513364112

Litasov, K. D., Shatskiy, A. F., & Ohtani, E. (2016). Interaction of Fe and Fe_3C with hydrogen and nitrogen at 6–20 GPa: A study by in situ X-ray diffraction. *Geochemistry International*, *54*(10), 914–921. https://doi.org/10.1134/S0016702916100074

Lodders, K. (2003). Solar system abundances and condensation temperatures of the elements. *The Astrophysical Journal*, *591*(2), 1220–1247. https://doi.org/10.1086/375492

Mao, W. L., Mao, H.-K., Sturhahn, W., Zhao, J., Prakapenka, V. B., Meng, Y., et al. (2006). Iron-rich post-perovskite and the origin of ultralow-velocity zones. *Science*, *312*(5773), 564–565. https://doi.org/10.1126/science.1123442

Marty, B. (2012). The origins and concentrations of water, carbon, nitrogen and noble gases on Earth. *Earth and Planetary Science Letters*, *313–314*, 56–66. https://doi.org/10.1016/j.epsl.2011.10.040

Marty, B., & Yokochi, R. (2006). Water in the early Earth. *Reviews in Mineralogy and Geochemistry*, *62*(1), 421–450. https://doi.org/10.2138/rmg.2006.62.18

Mason, B. (1963). The carbonaceous chondrites. *Space Science Reviews*, *1*(4), 621–646. https://doi.org/10.1007/BF00212446

McDonough, W. F. (2003). Compositional model for the Earth's core. In R. W. Carlson (Ed.), *Treatise on geochemistry*, (Vol. 2, pp. 547–568). Amsterdam: Elsevier. https://doi.org/10.1016/B0-08-043751-6/02015-6

McIntire, W. L. (1963). Trace element partition coefficients—A review of theory and applications to geology. *Geochimica et Cosmochimica Acta*, *27*(12), 1209–1264. https://doi.org/10.1016/0016-7037(63)90049-8

McNaughton, N. J., Borthwick, J., Fallick, A. E., & Pillinger, C. T. (1981). Deuterium-hydrogen ratios in unequilibrated ordinary chondrites. *Nature*, *294*(5842), 639–641. https://doi.org/10.1038/294639a0

Mizuno, H., Nakazawa, K., & Hayashi, C. (1980). Dissolution of the primordial rare gases into the molten Earth's material. *Earth and Planetary Science Letters*, *50*(1), 202–210. https://doi.org/10.1016/0012-821X(80)90131-4

Moore, G., Vennemann, T., & Carmichael, I. S. E. (1998). An empirical model for the solubility of H_2O in magmas to 3 kilobars. *American Mineralogist*, *83*(1-2), 36–42. https://doi.org/10.2138/am-1998-1-203

Morbidelli, A., Chambers, J., Lunine, J. I., Petit, J. M., Robert, F., Valsecchi, G. B., & et al. (2000). Source regions and timescales for the delivery of water to the Earth. *Meteoritics and Planetary Science*, *35*(6), 1309–1320. https://doi.org/10.1111/j.1945-5100.2000.tb01518.x

Morbidelli, A., Lunine, J. I., O'Brien, D. P., Raymond, S. N., & Walsh, K. J. (2012). Building terrestrial planets. *Annual Review of Earth and Planetary Sciences*, *40*(1), 251–275. https://doi.org/10.1146/annurev-earth-042711-105319

Mottl, M. J., Glazer, B. T., Kaiser, R. I., & Meech, K. J. (2007). Water and astrobiology. *Chemie der Erde*, *67*(4), 253–282. https://doi.org/10.1016/j.chemer.2007.09.002

O'Brien, D. P., Izidoro, A., Jacobson, S. A., Raymond, S. N., & Rubie, D. C. (2018). The delivery of water during terrestrial planet formation. *Space Science Reviews*, *214*(1), 47. https://doi.org/10.1007/s11214-018-0475-8

O'Brien, D. P., Morbidelli, A., & Levison, H. F. (2006). Terrestrial planet formation with strong dynamical friction. *Icarus*, *184*(1), 39–58. https://doi.org/10.1016/j.icarus.2006.04.005

Ohtani, E., Hirao, N., Kondo, T., Ito, M., & Kikegawa, T. (2005). Iron-water reaction at high pressure and temperature, and hydrogen transport into the core. *Physics and Chemistry of Minerals*, *32*(1), 77–82. https://doi.org/10.1007/s00269-004-0443-6

Ohtani, E., & Maeda, M. (2001). Density of basaltic melt at high pressure and stability of the melt at the base of the lower mantle. *Earth and Planetary Science Letters*, *193*(1-2), 69–75. https://doi.org/10.1016/S0012-821X(01)00505-2

Okuchi, T. (1997). Hydrogen partitioning into molten iron at high pressure: Implications for Earth's core. *Science*, *278*(5344), 1781–1784. https://doi.org/10.1126/science.278.5344.1781

Ormel, C. W., & Klahr, H. H. (2010). The effect of gas drag on the growth of protoplanets—Analytical expressions for the accretion of small bodies in laminar disks. *Astronomy and Astrophysics*, *520*(A43). https://doi.org/10.1051/0004-6361/201014903

Pepin, R. O. (1992). Origin of noble gases in the terrestrial planets. *Annual Review of Earth and Planetary Sciences*, *20*(1), 389–430. https://doi.org/10.1146/annurev.ea.20.050192.002133

Raymond, S. N., Quinn, T., & Lunine, J. I. (2004). Making other earths: Dynamical simulations of terrestrial planet formation and water delivery. *Icarus*, *168*(1), 1–17. https://doi.org/10.1016/j.icarus.2003.11.019

Raymond, S. N., Quinn, T., & Lunine, J. I. (2006). High-resolution simulations of the final assembly of Earth-like planets I. Terrestrial accretion and dynamics. *Icarus*, *183*, 265–282. https://doi.org/10.1016/j.icarus.2006.03.011

Raymond, S. N., Quinn, T., & Lunine, J. I. (2007). High-resolution simulations of the final assembly of Earth-like planets. 2. Water delivery and planetary habitability. *Astrobiology*, *7*(1), 66–84. https://doi.org/10.1089/ast.2006.06-0126

Ribas, Á., Bouy, H., & Merín, B. (2015). Protoplanetary disk lifetimes vs. stellar mass and possible implications for giant planet populations. *Astronomy and Astrophysics*, *576*(A52). https://doi.org/10.1051/0004-6361/201424846

Richet, P., Bottinga, Y., & Javoy, M. (1977). A review of H, C, N, O, S, and Cl stable isotope fractionation among gaseous molecules. *Annual Review of Earth and Planetary Sciences*, *5*(1), 65–110. https://doi.org/10.1146/annurev.ea.05.050177.000433

Robert, F. (2001). The origin of water on Earth. *Science*, *293*(5532), 1056–1058. https://doi.org/10.1126/science.1064051

Robert, F. (2003). The D/H ratio in chondrites. *Space Science Reviews*, *106*(1/4), 87–101. https://doi.org/10.1023/A:1024629402715

Robert, F. (2006). Solar system deuterium/hydrogen ratio. In D. S. Lauretta, & H. Y. McSween, Jr. (Eds.), *Meteorites and the early solar system II*, (pp. 341–351). Tucson, AZ: University of Arizona Press.

Rogers, L. A. (2015). *Most* 1.6 Earth-radius planets are not rocky. *The Astrophysical Journal*, *801*, 41. https://doi.org/10.1088/0004-637X/801/1/41

Rubie, D. C., Frost, D. J., Mann, U., Asahara, Y., Nimmo, F., Tsuno, K., et al. (2011). Heterogeneous accretion, composition and core-mantle differentiation of the Earth. *Earth and Planetary Science Letters*, *301*(1-2), 31–42. https://doi.org/10.1016/j.epsl.2010.11.030

Rubie, D. C., Jacobson, S. A., Morbidelli, A., O'Brien, D. P., Young, E. D., de Vries, J., et al. (2015). Accretion and differentiation of the terrestrial planets with implications for the compositions of early-formed solar system bodies and accretion of water. *Icarus*, *248*, 89–108. https://doi.org/10.1016/j.icarus.2014.10.015

Sarafian, A. R., Hauri, E. H., McCubbin, F. M., Lapen, T. J., Berger, E. L., Nielsen, S. G., et al. (2017). Early accretion of water and volatile elements to the inner solar system: Evidence from angrites. *Philosophical Transactions of the Royal Society A*, *375*(2094), 20160209. https://doi.org/10.1098/rsta.2016.0209

Sarafian, A. R., Nielsen, S. G., Marschall, H. R., McCubbin, F. M., & Monteleone, B. D. (2014). Early accretion of water in the inner solar system from a carbonaceous chondrite-like source. *Science*, *346*(6209), 623–626. https://doi.org/10.1126/science.1256717

Sasaki, S. (1990). Dissolution of primary solar-type atmosphere into the Earth's interior and terrestrial noble gas evolution. Lunar and Planetary Science Conference XXVIII, abstract #1606.

Schaefer, L., Jacobsen, S. B., Remo, J. L., Petaev, M. I., & Sasselov, D. D. (2017). Metal-silicate partitioning and its role in core formation and composition on super-Earths. *The Astrophysical Journal*, *835*(2), 234. https://doi.org/10.3847/1538-4357/835/2/234

Scheinberg, A., Elkins-Tanton, L. T., & Zhong, S. J. (2014). Timescale and morphology of Martian mantle overturn immediately following magma ocean solidification. *Journal of Geophysical Research: Planets*, *119*, 454–467. https://doi.org/10.1002/2013JE004496

Scherstén, A., Elliott, T., Hawkesworth, C., Russell, S., & Masarik, J. (2006). Hf-W evidence for rapid differentiation of iron meteorite parent bodies. *Earth and Planetary Science Letters*, *241*(3-4), 530–542. https://doi.org/10.1016/j.epsl.2005.11.025

Schlichting, H. E., Ofek, E. O., Wenz, M., Sari, R., Gal-Yam, A., Livio, M., et al. (2009). A single sub-kilometre Kuiper belt object from a stellar occultation in archival data. *Nature*, *462*(7275), 895–897. https://doi.org/10.1038/nature08608

Schneider, D. M., Benoit, P. H., Kracher, A., & Sears, D. W. G. (2003). Metal size distributions in EH and EL chondrites. *Geophysical Research Letters*, *30*(8), 1420. https://doi.org/10.1029/2002GL016672

Schnetzler, C. C., & Philpotts, J. A. (1971). Alkali, alkaline earth and rare-earth element concentrations in some Apollo 12 soils, rocks, and separated phases. *Proceedings of the Lunar Science Conference*, *2*, 801–837.

Sharp, Z. D. (2017). Nebular ingassing as a source of volatiles to the terrestrial planets. *Chemical Geology*, *448*, 137–150. https://doi.org/10.1016/j.chemgeo.2016.11.018

Shibazaki, Y., Ohtani, E., Terasaki, H., Suzuki, A., & Funakoshi, K. (2009). Hydrogen partitioning between iron and ringwoodite: Implications for water transport into the Martian core. *Earth and Planetary Science Letters*, *287*(3-4), 463–470. https://doi.org/10.1016/j.epsl.2009.08.034

Solomatov, V. S. (2000). Fluid dynamics of a terrestrial magma ocean. In R. M. Canup, & K. Righter (Eds.), *Origin of the Earth and Moon*, (pp. 323–338). Tucson, AZ: University of Arizona Press.

Stökl, A., Dorfi, E., & Lammer, H. (2015). Hydrodynamic simulations of captured protoatmospheres around Earth-like planets. *Astronomy and Astrophysics*, *576*, A87. https://doi.org/10.1051/0004-6361/201423638

Tang, H., & Dauphas, N. (2014). ^{60}Fe–^{60}Ni chronology of core formation in Mars. *Earth and Planetary Science Letters*, *390*, 264–274. https://doi.org/10.1016/j.epsl.2014.01.005

Terasaki, H., Shibazaki, Y., Nishida, K., Tateyama, R., Takahashi, S., Ishii, M., et al. (2014). Repulsive nature for hydrogen incorporation to Fe_3C up to 14 GPa. *ISIJ International*, *54*(11), 2637–2642. https://doi.org/10.2355/isijinternational.54.2637

Tonks, W. B., & Melosh, H. J. (1993). Magma ocean formation due to giant impacts. *Journal of Geophysical Research*, *98*(E3), 5319–5333. https://doi.org/10.1029/92JE02726

Touboul, M., Kleine, T., Bourdon, B., Palme, H., & Wieler, R. (2007). Late formation and prolonged differentiation of the Moon inferred from W isotopes in lunar metals. *Nature*, *450*(7173), 1206–1209. https://doi.org/10.1038/nature06428

Umemoto, K., & Hirose, K. (2015). Liquid iron-hydrogen alloys at outer core conditions by first-principles calculations. *Geophysical Research Letters*, *42*, 7513–7520. https://doi.org/10.1002/2015GL065899

Villeneuve, J., Chaussidon, M., & Libourel, G. (2009). Homogeneous distribution of ^{26}Al in the solar system from the Mg isotopic composition of chondrules. *Science*, *325*(5943), 985–988. https://doi.org/10.1126/science.1173907

Wade, J., & Wood, B. J. (2005). Core formation and the oxidation state of the Earth. *Earth and Planetary Science Letters*, *236*(1-2), 78–95. https://doi.org/10.1016/j.epsl.2005.05.017

Warren, P. H. (2011). Stable-isotopic anomalies and the accretionary assemblage of the Earth and Mars: A subordinate role for carbonaceous chondrites. *Earth and Planetary Science Letters*, *311*(1-2), 93–100. https://doi.org/10.1016/j.epsl.2011.08.047

Weidenschilling, S. J. (2000). Formation of planetesimals and accretion of the terrestrial planets. *Space Science Reviews*, *92*(1/2), 295–310. https://doi.org/10.1023/A:1005259615299

Weinstein, M., & Elliott, J. F. (1963). Solubility of hydrogen in liquid iron alloys. *Transactions of the Metallurgical Society of the American Institute of Mechanical Engineers*, *227*, 382–393.

Weiss, L. M., & Marcy, G. W. (2014). The mass-radius relation for 65 exoplanets smaller than 4 Earth radii. *The Astrophysical Journal Letters*, *783*(1), L6. https://doi.org/10.1088/2041-8205/783/1/L6

Wood, B. J., Li, J., & Shahar, A. (2013). Carbon in the core: Its influence on the properties of core and mantle. *Reviews in Mineralogy and Geochemistry*, *75*(1), 231–250. https://doi.org/10.2138/rmg.2013.75.8

Wood, B. J., Walter, M. J., & Wade, J. (2006). Accretion of the Earth and segregation of its core. *Nature*, *441*(7095), 825–833. https://doi.org/10.1038/nature04763

Yokochi, R., & Marty, B. (2004). A determination of the neon isotopic composition of the deep mantle. *Earth and Planetary Science Letters*, *225*(1-2), 77–88. https://doi.org/10.1016/j.epsl.2004.06.010

Yoshino, T., Walter, M. J., & Katsura, T. (2003). Core formation in planetesimals triggered by permeable flow. *Nature*, *422*(6928), 154–157. https://doi.org/10.1038/nature01459

Youdin, A. N., & Goodman, J. (2005). Streaming instabilities in protoplanetary disks. *The Astrophysical Journal*, *620*(1), 459–469. https://doi.org/10.1086/426895

Zaranek, S. E., & Parmentier, E. M. (2004). The onset of convection in fluids with strongly temperature-dependent viscosity cooled from above with implications for planetary lithospheres. *Earth and Planetary Science Letters*, *224*(3-4), 371–386. https://doi.org/10.1016/j.epsl.2004.05.013

Zhang, Y., & Yin, Q.-Z. (2012). Carbon and other light element contents in the Earth's core based on first-principles molecular dynamics. *Proceedings of the National Academy of Sciences of the United States of America*, *109*(48), 19579–19583. https://doi.org/10.1073/pnas.1203826109